Preprints.org

Article

Not peer-reviewed version

Limited Local Clinical Trials for the New Cancer Treatment Technology Karanahan for Patients with Advanced Breast Cancer

Veronika A Markina , Anastasia S Proskurina , Vera S Ruzanova , Genrikh S Ritter , Evgeniya V Dolgova , Svetlana S Kirikovich , Evgeniy V Levites , Sofya G Oshihmina , Yaroslav R Efremov , Eugene I Vereschagin , Olga Y Leplina , Alexandr A Ostanin , Elena R Chernykh , Nikolay A Kolchanov , Sergey V Sidorov , Sergey S Bogachev *

Posted Date: 25 September 2024

doi: 10.20944/preprints202409.2002.v1

Keywords: breast cancer; cyclophosphamide; double-stranded DNA; palliative patients

Preprints.org is a free multidiscipline platform providing preprint service that is dedicated to making early versions of research outputs permanently available and citable. Preprints posted at Preprints.org appear in Web of Science, Crossref, Google Scholar, Scilit, Europe PMC.

Copyright: This is an open access article distributed under the Creative Commons Attribution License which permits unrestricted use, distribution, and reproduction in any medium, provided the original work is properly cited.

Preprints.org (www.preprints.org) | NOT PEER-REVIEWED | Posted: 25 September 2024 doi:10.20944/preprints202409.2002.v

Disclaimer/Publisher's Note: The statements, opinions, and data contained in all publications are solely those of the individual author(s) and contributor(s) and not of MDPI and/or the editor(s). MDPI and/or the editor(s) disclaim responsibility for any injury to people or property resulting from any ideas, methods, instructions, or products referred to in the content.

Article

Limited Local Clinical Trials for the New Cancer Treatment Technology Karanahan for Patients with Advanced Breast Cancer

Veronika A Markina [1,#], Anastasia S Proskurina [2,#], Vera S Ruzanova [2], Genrikh S Ritter [2], Evgeniya V Dolgova [2], Svetlana S Kirikovich [2], Evgeniy V Levites [2], Sofya G Oshikhmina [1,2], Yaroslav R Efremov [1,2], Eugene I Vereschagin [3], Olga Y Leplina [4], Alexandr A Ostanin [4], Elena R Chernykh [4], Nikolay A. Kolchanov [2], Sergey V Sidorov [1,5,#] and Sergey S Bogachev [2,*,#]

[1] Novosibirsk National Research State University, Novosibirsk 630090, Russia
[2] Institute of Cytology and Genetics of the Siberian Branch of the Russian Academy of Sciences, Novosibirsk 630090, Russia
[3] Novosibirsk State Medical University, Novosibirsk 630091, Russia
[4] Research Institute of Fundamental and Clinical Immunology, Novosibirsk 630099, Russia
[5] Oncology Department, Municipal Hospital No 1, Novosibirsk 630047, Russia
* Correspondence: labmolbiol@mail.ru
[#] These authors contributed equally to this work

Abstract: (1) Background: Multi-year research into the synergistic effect of cyclophosphamide and complex composite double-stranded DNA preparation (DNAmix) has made it possible to develop the novel *Karanahan* technology for treating malignant tumors, which is based on the eradication of cancer stem cells; (2) Methods: Pilot clinical trials for *Karanahan* technology were conducted in 12 patients with advanced stage IV breast cancer; (3) Results: The findings indicate that the analyzed treatment regimen ensures a local positive therapeutic response, significantly increases patient survival time, and activates the adaptive antitumor immune response. Adjustment of the basic regimen of *Karanahan* technology has been developed, which consists of increasing the dose of the DNAmix complex composite double stranded DNA preparation and its lymphotropic administration to the main lymph depots simultaneously with intratumoral injection; (4) Conclusions: *Karanahan* technology has a promising therapeutic potential in the treatment of inoperable stage IV breast cancer.

Keywords: breast cancer; cyclophosphamide; double-stranded DNA; palliative patients

1. Introduction

In modern oncology, there exist two fundamentally different cancer treatment options: the curative and the palliative ones [1–3]. At non-advanced cancer stages, when there is a real chance that a patient will be completely cured, all therapy measures that aim to combat this pathological process are regarded as curative treatment options. Palliative treatment is used in advanced stages, when patients have virtually no chances for compete recovery [4–8].

Globally, there are more than 25 million cancer patients who belong to the palliative cohort; ~ 18% of these patients have breast cancer; ~ 12%, colon cancer; and ~10%, prostate cancer. The relationship between the number of diagnosed patients and those surviving for at least 5 years is a prognostic marker of overall survival. Thus, this ratio is 3.8 for breast cancer; 2.7, for colon cancer; 1.5 for stomach cancer; and 1.0, for lung cancer [9].

Palliative chemotherapy is used with a deliberately nonradical objective for incurable patients with regional or distant spread of inoperable tumor processes. Meanwhile, palliative chemotherapy can increase the survival time of patients with types of spread cancers by several months or even

© 2024 by the author(s). Distributed under a Creative Commons CC BY license.

Preprints.org (www.preprints.org) | NOT PEER-REVIEWED | Posted: 25 September 2024 doi:10.20944/preprints202409.2002.v

years [3,8–15]. It is conventionally assumed that when talking about solid chemosensitive tumors such as breast cancer, ovarian cancer, lung cancer, and colorectal cancer, the term 'incurable' is used when distant metastases are present (stage IV) and, in some cases, when there is an inoperable regional metastatic process (stage IIIB for lung cancer) [16,17]. Patients' expected survival time plays almost no role in these cases. In patients with distant metastases, even if their functional status is satisfactory and the survival time can potentially be five years and even longer, the disease is considered incurable [18]. It does not actually matter how long a patient will survive; what is important is that there are no chances of cure. In other words, if the probability that a patient eventually dies of current cancer is very high, the disease is considered incurable regardless of how long he or she stays alive [19].

Palliative chemotherapy aims to improve patient quality of life and survival time. However, it sometimes does not increase survival time compared to maintenance therapy and is highly dependent on the type and stage of cancer [20].

A typical feature of chemotherapy for patients with advanced cancer is that it does not involve a certain finite number of cycles. This therapy is given indefinitely as long as it helps curb the disease and does not cause serious adverse events. Tumor response to treatment is determined according to the RECIST guideline (version 1.1). Reduction in tumor size, attaining temporary remission, stabilization, or inhibition of the progression of the pathological process are sufficient to achieve the aforementioned objectives [18,21,22].

The challenge of decision making when performing palliative chemotherapy consists of ensuring the balance between quality of life and survival. In other words, the adverse symptoms of chemotherapy should not be a greater burden for the patient than the symptoms of the disease per se. Currently, there are no uniform standardized criteria for selecting cancer patients to receive palliative chemotherapy. For most tumors, details of the application of chemotherapy (indications to prescribe a particular antitumor agent or their combinations, administration procedure, and doses), rather than its appropriateness and effectiveness, are a matter of discussion. The key practical challenge of chemotherapy is associated with the details and methodology of its application [23]. One of the well-known features of chemotherapy is that there are no unified generally accepted treatment protocols for all tumor types [13,18]. There is even less certainty about palliative care for cancer patients, for which the objectives are quite different, as already mentioned. The age and poor general condition of patients with inoperable advanced cancer limits pharmacological therapy options and is often the reason why treatment is not performed at all [18]. Therefore, the most challenging problem in palliative chemotherapy is choosing the optimal treatment strategy to solve the dilemma of how to conduct effective therapy while avoiding toxic effects. To have a high quality of life for patients, key clinical manifestations of metastatic cancer must be reduced, which is possible only through effective chemotherapy that in turn causes a number of unwanted adverse effects. In pursuit of the mandatory balance between the manifestations of the disease per se and the side symptoms of treatment, in most cases the attending oncologist/chemotherapist performs personified correction of therapy regimens, since no definite criteria or techniques for modifying palliative chemotherapy regimens are currently available [19].

Cyclophosphamide (CP) is an alkylating chemotherapeutic agent that belongs to the oxazaphosphorine group. On exposure to cytochrome P450, it forms cytotoxic metabolites in the liver. CP is widely used in palliative therapy. In palliative chemotherapy using CP, the cytostatic is most effective when used in the low-dose metronomic regimen, or as monotherapeutic or in combination with other cytostatic agents. Metronomic chemotherapy is potentially a less toxic but quite effective treatment strategy, being a novel, active, and well-tolerated therapeutic modality for patients with advanced tumors [24].

Metronomic CP is a chemotherapeutic agent that is most commonly studied in preclinical experimental research [25,26]. Thus, it has been demonstrated in animal models that metronomic administration of CP repolarizes M2-like tumor-associated macrophages toward the tumor-suppressive M1 phenotype, selectively reduces the number of circulating CD4+CD25+ regulatory T cells, while restoring the effector functions of T cells and natural killer cells, thus ensuring better

Preprints.org (www.preprints.org) | NOT PEER-REVIEWED | Posted: 25 September 2024 doi:10.20944/preprints202409.2002.v

control over the disease [27]. Recent studies have demonstrated that metronomic chemotherapy using low-dose CP activates cytotoxic CD8+ T cells and can induce long-term immunological memory, manifested as rejection of the tumor grafted in GL261 mouse glioma models [28]. In clinical practice, this approach has been approved for treating patients with metastatic breast cancer [29,30]. It was demonstrated that therapy reduced the count of circulating regulatory T cells by 40% ($p = 0.002$), while the count of tumor-specific effector T cells increased statistically significantly ($p = 0.03$). This immunomodulatory effect was directly correlated with stabilization of the disease and overall survival of the patients ($p < 0.05$). Metronomic chemotherapy has been included in the Updated Guidelines of the German expert group "AGO Breast Committee" where metronomic therapy is recommended for patients with HR-positive, HER2-negative metastatic breast cancer who had previously received anthracycline–taxane chemotherapy.

Multi-year research into the synergistic effect of CP cytostatic and complex composite double-stranded DNA preparation (DNAmix) has made it possible to develop the novel *Karanahan* technology for treating malignant tumors, which is based on the eradication of cancer stem cells. The *Karanahan* technology has been thoroughly described in refs. [31,32]. This approach is of chronometric nature and implies the administration of both CP and DNAmix in strict dependence on the duration of DNA repair and the cell cycle pattern of each particular tumor. After being applied, the technology results in the eradication of cancer stem cells and the induction of extensive apoptosis of committed cancer cells. The technology has been tested in different experimental murine tumor models: Krebs-2 ascites and solid carcinoma [33,34], hepatocellular carcinoma (G-29) with ascites [35], RLS lymphosarcoma [36], Lewis carcinoma [31], A20 lymphoma [37], as well as human tumor models: U87 glioblastoma [38] and primary glioblastoma cultures [39].

Low-dose metronomic chemotherapy with CP and *Karanahan* technology have the same chronometric platform for CP administration and therapeutic direction [40]. Both treatment modalities reduce the pro-tumor activity of the tumor-associated stroma and activate the anti-tumor immune response. It is accompanied by complete regression of the nidus of immunogenic tumors in the case of low-dose metronomic chemotherapy with CP and nidi of primary tumors, both immunogenic and nonimmunogenic, in the case of using *Karanahan* technology in experimental animals [37]. Nonetheless, eradication of cancer stem cells rather than the antitumor immune response is the pivotal event in *Karanahan* technology that predetermines curing of mice grafted with tumor of any genesis. Furthermore, the addition of DNAmix to therapy induces extensive apoptosis of committed cancer cells [33], thus reducing the tumor load and therefore increasing the overall therapeutic potential of treatment. This comparison gives grounds for suggesting that *Karanahan* technology can be used as an option of palliative chemotherapy with CP having new therapeutic characteristics, namely the possibility of eliminating cancer stem cells from the tumor nidus and simultaneous induction of extensive apoptosis of tumor tissue cells. As it ensures stimulation of the antitumor immune response and reduces protumor activity of the tumor-associated stroma, this approach can be a potent therapeutic tool for patients with advanced cancer and stage IV breast cancer in particular.

In the present study, the novel technology for the treatment of malignant neoplasms, which had previously been tested in experimental animals, was used in a local clinical trial as a therapeutic procedure for the palliative treatment of advanced breast cancer.

2. Materials and Methods

2.1. The MCF-7 Cell Culture

Cells were cultured in DMEM supplemented with 10% FBS and 100 μg/mL gentamicin antibiotic. After triple exposure of cells to 1 μg/mL mitomycin C (Sigma, USA) once daily (days 3 through 10 after the first exposure to mitomycin C), a sample of MCF-7 cells was collected. Half of the cells were fixed in an equal volume of methanol to analyze the cell cycle distribution according to propidium iodide fluorescence and identify the cell synchronization time. The remaining cells were incubated with 0.1 μg of TAMRA-labeled DNA probe in the dark at room temperature; then they were washed and deposited onto slides by cytospinning, coated with DAPI/DABCO under the

Preprints.org (www.preprints.org) | NOT PEER-REVIEWED | Posted: 25 September 2024 doi:10.20944/preprints202409.2002.v

coverslip; the count of TAMRA+ cells was evaluated on a Zeiss Axio Imager M2 fluorescence microscope.

2.2. Clinical Study

A clinical study of personalized chemotherapy for breast cancer with low doses of cyclophosphamide (NCT06361264) was conducted. The study was approved by the Local Ethics Committee of the Research Institute of Fundamental and Clinical Immunology. The study was carried out in accordance with the Declaration of Helsinki of the World Medical Association. Written informed consent to participate in the study was obtained from each of the patients, which specified open publication of the results presented as reports or otherwise.

Patients had stage IV breast cancer or disease progression with the presence of foci accessible for biopsy of tumor material. Tumor samples were handled according to the procedure described in ref. [32]. Primary cultures were obtained; TAMRA+ cells were counted. The duration of the DNA repair process and the time of cell synchronization after three exposures to mitomycin C were determined. The CP administration schedule was determined for each patient according to the resulting time points.

According to the elaborated regimen, patients received 4 intravenous cyclophosphamide injections at the dose of 300 mg/m^2 in combination with 4 injections of 1-12 mg of DNAmix administered to prominent tumor nidi and lymph depots. The patients received 2 to 6 courses of therapy. The interval between courses was 21 days.

2.3. An Obligatory Comment for Schedule Determination

Calculating the repair cycle time starts at the point where the number of double-strand breaks is minimal. If this value is minimal at the zero point, the calculation starts at the zero point. The reason is that active transcription occurs in tumor cells, giving rise to transient double-strand breaks that are detected by the comet assay at the zero point. It is the minimal number of double-strand breaks after transcriptional pausing that means that the transcriptional activity of the cell has been paused and double-strand repair (i.e., the DNA repair cycle) has started. Therefore, the first time interval of the repair cycle involves all the time until the second minimal number of double-strand breaks. The time interval of the true DNA repair cycle starts with the first minimal number of double strand breaks and ends with the second minimum. This interval is included in the schedule after the first treatment is extended by the time it takes for transcriptional activity to end.

Why does triple exposure to CP lead to cell cycle synchronization of cancer stem cells? The repair time for different chromosome regions is related to the presence of repetitive DNA in them. The repair dynamics looks as follows. Double-strand breaks in euchromatin are repaired first, followed by repair of double-strand breaks in intercalary heterochromatin and possibly telomeres; finally, the repair machinery fixes double-strand breaks in centromeric heterochromatin. The multiple number of sites to be repaired, in combination with spatial hindrance to the molecular repair machinery in centromeric heterochromatin, are the possible reasons for the synchronization of the DNA repair machinery in different cells. At the initial repair stage, all easily accessible sites bind to the DNA repair complex and are fixed. Centromeric heterochromatin remains a region that is difficult to access for repair; as suggested earlier, the kinetics of binding of the repair machinery to sites within this region is low. In other words, all the energy was originally put into the repair of easily accessible sites. Once DNA repair at easily accessible sites is completed, all the DNA repair complexes simultaneously reach the sites in centromeric heterochromatin. The number of these complexes apparently is equal to or greater than the number of sites to be repaired. All the breaches are closed synchronously. This situation is obviously dependent on the cytostatic doses and the number of interstrand crosslinks induced by them.

2.4. Patients

Table 1. Study participants.

Preprints.org (www.preprints.org) | NOT PEER-REVIEWED | Posted: 25 September 2024 doi:10.20944/preprints202409.2002.v

Patient No.	Year of birth	Regimen	Chemotherapy courses performed (start date)	Date of death
1	1960	CP 0 hrs – 28 hrs – 56 hrs – 132 hrs DNA 22 hrs after CP	Nov. 9, 2018 Nov. 28, 2018	-
1-2	1960	CP 0 hrs – 46 hrs – 92 hrs – 192 hrs DNA 24 hrs after CP	Dec. 15, 2021 Jan. 12, 2022 Feb. 7, 2022	March 2023
2	1971	CP 0 hrs – 46 hrs – 92 hrs – 192 hrs DNA 30 hrs after CP	Oct. 9, 2019 Nov. 13, 2019 Dec. 9, 2019	March 2020
3	1959	CP 0 hrs – 46 hrs – 92 hrs – 156 hrs DNA 24 hrs after CP	Jan. 25, 2021 Feb. 15, 2021 March 5, 2021	December 2022
4	1949	CP 0 hrs – 42 hrs – 84 hrs – 168 hrs DNA 36 hrs after CP	April 8, 2021 April 30, 2021 May 24, 2021	April 2023
5	1959	CP 0 hrs – 34 hrs – 68 hrs – 216 hrs DNA 30 hrs after CP	May 11, 2021 June 1, 2021 June 29, 2021 Nov. 24, 2021 Dec. 15, 2021 Jan. 12, 2022	May 2023
6	1956	CP 0 hrs – 34 hrs – 68 hrs – 106 hrs – 192 hrs DNA 30 hrs after CP	Nov. 16, 2021 Dec. 7, 2021	May 2022
7	1982	CP 0 hrs – 40 hrs – 80 hrs – 144 hrs DNA 30 hrs after CP	April 19, 2022 May 16, 2022	July 2022
8	1950	CP 0 hrs – 16 hrs – 32 hrs – 72 hrs DNA 12 hrs after CP	April 20, 2022 May 16, 2022	June 2022
9	1962	CP 0 hrs – 34 hrs – 56 hrs – 120 hrs DNA 24 hrs after CP DNA 12 hrs after CP	March 3, 2023 April 4, 2023 June 2, 2023 Aug. 16, 2023	August 2023
10	1971	CP 0 hrs – 16 hrs – 26 hrs – 144 hrs DNA 12 hrs after CP DNA 6 hrs after CP	May 24, 2023 June 2, 2023 July 26, 2023	
11	1975	CP 0 hrs – 16 hrs – 26 hrs – 144 hrs DNA 12 hrs after CP DNA 6 hrs after CP	May 24, 2023 July 26, 2023	
12	1976	CP 0 hrs – 16 hrs – 26 hrs – 144 hrs DNA 12 hrs after CP DNA 6 hrs after CP	June 2, 2023 July 26, 2023 Aug. 12, 2023	
		CP 0 hrs – 40 hrs – 52 hrs – 144 hrs DNA 36 hrs after CP DNA 6 hrs after CP	Sept.11, 2023 Oct. 9, 2023	

2.5. Assessment of Regulatory T Cells and CD8 T-Cell Population in Patients' Peripheral Blood

Preprints.org (www.preprints.org) | NOT PEER-REVIEWED | Posted: 25 September 2024 doi:10.20944/preprints202409.2002.v

Regulatory T cells were quantified by flow cytometry on a FACSCalibur flow cytometer (BectonDickinson, USA) using anti-CD4, anti-CD25, and anti-FOXP3 monoclonal antibodies (BD PharMingen, USA).

Externalization of CD107a on the surface of CD8 T cells was assessed using a degranulation assay. Mononuclear cells were incubated in the presence of anti-CD107a antibodies, monensin, and anti-CD3 antibodies as a T-cell stimulator. Anti-CD3 antibodies were not added to the control. After 18 hours, cells were incubated with anti-CD8 antibodies according to the standard procedure for detecting cell surface antigens. The level of CD107a expression was determined on a flow cytometer at the CD8 cell gate.

2.6. Statistical Analysis

Statistical analysis was performed using Statistica 8 software (StatSoft, USA). The validity of the differences was evaluated using the Mann-Whitney U test. The differences revealed were considered statistically significant at $p < 0.05$.

3. Results

The study involved two stages. In the first stage, we analyzed the effect of *Karanahan* technology on MCF-7 cell culture as a common breast cancer model. This stage was needed to prove the efficacy of breast cancer therapy in a cell model. The second stage involved limited local clinical trials aimed at assessing the safety, tolerability, and efficacy of *Karanahan* technology in palliative patients with incurable metastatic breast cancer. The control cohort consisted of historical control patients who had the matched stage of tumor progression.

3.1. The Effect of Karanahan Technology on Changes in the Size of Cancer Stem Cell Population and Viability of MCF-7 Breast Cancer Cells

Diagnostic analysis of *Karanahan* technology involves evaluation of the cellular repair cycle and distribution of cells by phases of the cell cycle after exposure to a cross-linking cytostatic agent in accordance with the identified time parameters of the repair cycle. To analyze the DNA repair cycle in MCF-7 cell culture, cells were treated with the direct-acting crosslinking cytostatic agent mitomycin C. After the maximum accumulation of double-strand breaks had been found (Figure 1A), cells were exposed to the mitomycin C cytostatic agent three times in a 22 hour interval (Figure 1B). The cell distribution in the phases of the cell cycle was analyzed within 10 days after the first cytostatic treatment. The final treatment point for MCF-7 cells (according to the *Karanahan* technology procedure) was chosen to be 6 days after the first cytostatic treatment (Figure 1C).

Efficacy against cancer stem cells is one of the key parameters that characterize *Karanahan* technology. In our earlier study [32], we demonstrated that TAMRA+ breast cancer cells substantially overlap with conventional breast cancer markers and are cancer stem cells in patients with this disease. Hence, we quantified changes in the percentage of TAMRA+ cells and therefore MCF-7 cancer stem cells throughout treatments (Figure 1D). The percentage of cells was found to reach the minimal value on day 6 and then increase abruptly. This value is as expected, since massive apoptosis of committed cells is induced at this time, and the relative percentage of apoptosis-resistant cells (cancer stem cells being among them) will obviously increase. Furthermore, once cancer stem cells complete repair, they proceed to division, which also contributes to the increase in the percentage of TAMRA+ cells.

DNAmix, which is the cornerstone of *Karanahan* technology, was not supposed to be added to the therapy protocol. The effect of DNAmix was repeatedly evaluated in similar experiments for cancer cell cultures and did not require mandatory validation.

Preprints.org (www.preprints.org) | NOT PEER-REVIEWED | Posted: 25 September 2024 doi:10.20944/preprints202409.2002.v

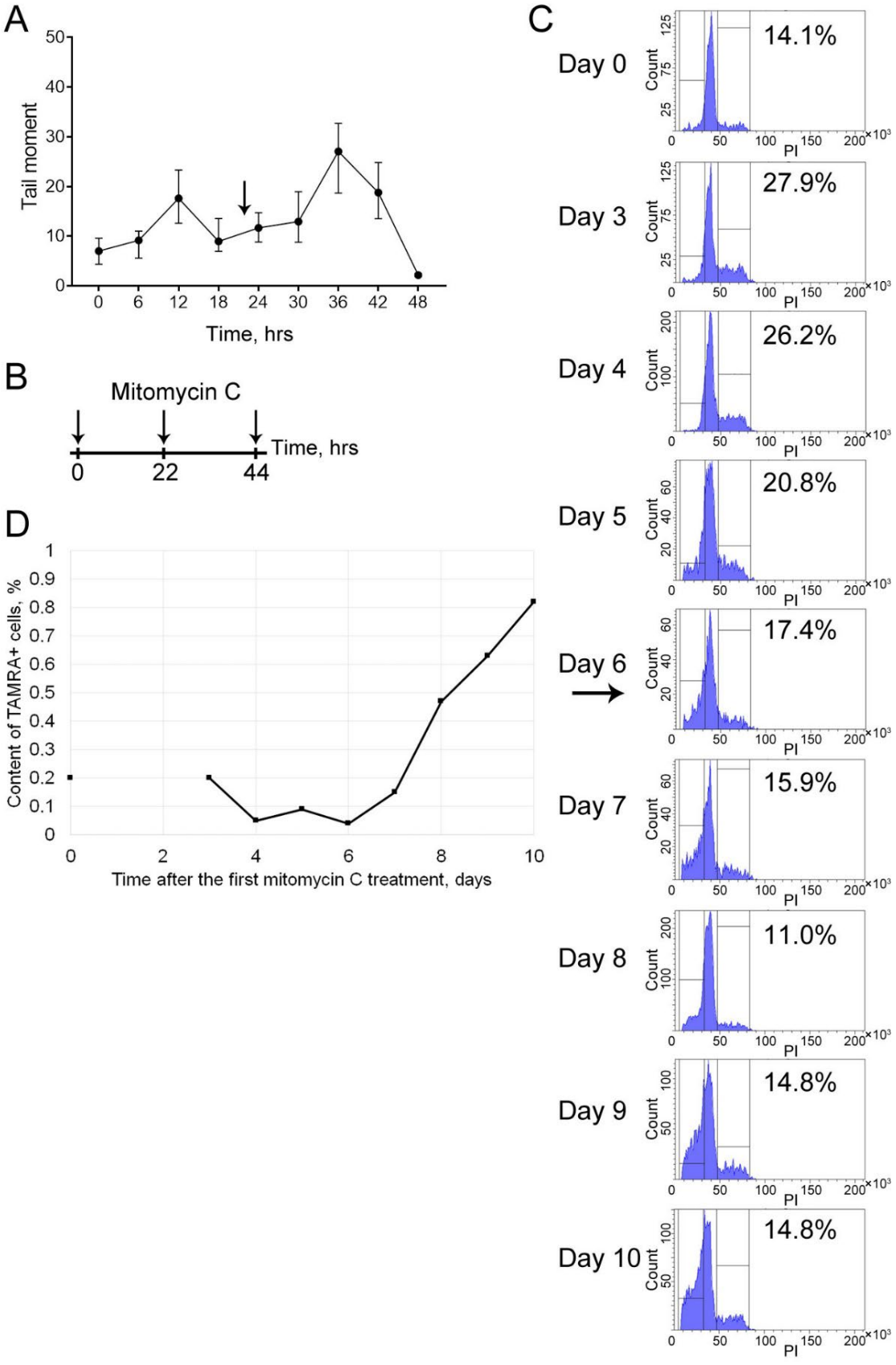

Figure 1. (A) The DNA repair cycle in MCF-7 cell culture. (B) Scheme of treating MCF-7 cells with mitomycin C. (C) The cell cycle of MCF-7 cells after triple treatment with mitomycin C. (D) The percentage of TAMRA+ cancer stem cells in MCF-7 cell culture after triple treatment with mitomycin C.

Preprints.org (www.preprints.org) | NOT PEER-REVIEWED | Posted: 25 September 2024 doi:10.20944/preprints202409.2002.v

The findings demonstrated that breast cancer cells, both committed and TAMRA+ cancer stem cells, were sensitive to *Karanahan* technology and that this technology can be applied in clinical practice under experimental conditions for incurable palliative patients who have the terminal stage of the disease.

3.2. The Results of Limited Pilot Clinical Trials of Karanahan Technology

A clinical trial protocol was developed. The general methodology of *Karanahan* technology is as follows [32]. During the preparatory stage, a tumor sample is harvested intraoperatively. The primary culture is obtained from this tumor tissue sample. The number of cancer stem cells is quantified according internalization of the TAMRA+ DNA probe. The repair cycle time is then estimated, and the day the tumor cells are synchronized in the G2 / M cell cycle phase is identified. The schedules for administering CP and DNAmix are calculated according to the resulting time points. The schedule is handed to the physician in charge and therapy is performed. According to the elaborated regimen, CP is administered intravenously, while DNAmix is injected into lymph node depot areas in inguinal and axillary lymph node clusters, the abdominal lymph node 5 cm to the right of the umbilicus (paraumbilically) and into prominent tumor nidi (Supplementary Materials 1, 2).

The objective of the present clinical trial was not complete curation of stage IV breast cancer patients like it was for the experimental mouse models. The primary objective of the study was to test the applicability of *Karanahan* technology in humans in a real-world clinical setting. We needed to understand whether the technology works in a clinical setting, what drawbacks it has, and what are the hidden pitfalls for this therapeutic approach. In this regard, the key criterion for assessing the efficacy of *Karanahan* technology was the response of the primary tumor nidus to therapy and the survival time of palliative patients.

3.2.1. Results of Karanahan Therapy in Patients

At the time when the results were reported, 12 palliative patients diagnosed with stage IV breast cancer had participated in the study (Figure 2). The patients received two to six therapy courses using *Karanahan* technology. Several patients were withdrawn from the study due to treatment-induced active catabolic processes (active necrosis with massive rejection; severe hyperemia) in the tumor subjected to therapy (the detoxification procedure was developed and used beginning with the fourth *Karanahan* therapy course in patient 12, Supplementary Material 2).

The results are individually reported for the cases included in the study. The analysis of the results consists of two sections. The first section involves the data from laboratory examination of the *Karanahan* technology indicators and provides an illustration of changes that occur within the primary tumor site (photographs) during treatment (Figures 2–14). In the second section, data describing the occurring changes are collected and summarized in a table (Supplementary Material 3). Since all patients had metastases of different localization and the effect of treatment could refer to all affected areas, the efficacy of treatment was evaluated with account for the response observed in all nidi affections. Three response categories were selected: favorable response, no response, and unfavorable response. The table lists descriptions of changes according to response categories with allowance for all nidi of tumor dissemination according to the results of the specified instrumental analyzes on specified dates after treatment.

The results for patient 1 were used for analysis twice and labeled entries Nos. 1 and 1-2. That was because after two courses of treatment using *Karanahan* technology, tumor nidi in patient 1 was completely eliminated and no signs of tumor growth were observed for 2.5 years. However, after 3 years, this patient was readmitted for treatment, labeled entry No. 1-2. Tumor cell parameters were again evaluated and therapy was performed with the new regimen. We found it reasonable to analyze these two cases separately.

The following amendments were made and additional analyzes were performed throughout the study.

Patient 9. After the third course of therapy, biopsy material from the tumor area was analyzed to determine whether tumor cells were present; the schedule was supposed to then be adjusted. The

Preprints.org (www.preprints.org) | NOT PEER-REVIEWED | Posted: 25 September 2024 doi:10.20944/preprints202409.2002.v

tumor stroma sample did not contain a noticeable amount of tumor cells or any other cells. Of course, no trace of TAMRA+ cancer stem cells was detected. This fact, like in the case of experimental mouse models, indicates that treatment using the *Karanahan* technology is accompanied by fundamental positive changes in the tumor-associated stroma of the primary nidus. Tumor cells, including cancer stem cells, disappear, and only fibrous tissue remains.

Patient 12. The biological status of the cell populations in the pleural fluid was evaluated after three therapy courses. Cells in carcinoma nidus were found to have acquired a clear timing of DNA repair with a single dominant peak. The schedule was adjusted to account for the new findings. Furthermore, the dose of DNAmix administered increased from 1 to 12 mg per treatment session. Finally, in order to increase the chances of delivering DNA to the target metastatic nidus in the liver, peritoneum, and thoracic lymph nodes, we started to inject DNAmix into lymph depot areas in inguinal and axillary lymph node clusters, the abdominal lymph depot 5 cm to the right of the umbilicus (paraumbilically), and into prominent tumor nidi (Supplementary Material 2). After adjustment of the procedure, the pleural effusion decreased in both terms of volume and frequency of evacuation (30 days vs. 2–4 days between evacuations).

Table 2 summarizes the general conclusions about the results of *Karanahan* therapy for all patients.

Table 2. The general conclusions for the entire therapy.

Patient No.	Number of courses		Positive dynamics	No dynamics	Negative dynamics
1	2	*Local*	Elimination of metastases to temporal bone and soft tissues of the inguinal region		
		Systemic	Elimination of tumor nidus in the liver		
1-2	3	*Local*		Persistence of grade 1–2 postoperative lymphedema in the left breast and left upper limb	
		Systemic	Elimination of a single small nidus in the S6 segment of the right lung		Leukopenia. Growth of neoplasms in the liver
2	3	*Local*	Left breast: tumor diameter decreased by ~ 30% Right breast: tumor diameter decreased by ~ 50%		
		Systemic	Partial necrosis of hepatic metastases	Stabilization of hepatic metastatic disease	Progression of spinal metastases
3	3	*Local*	Reduced intensity of ipsilateral skin-affecting		

Preprints.org (www.preprints.org) | NOT PEER-REVIEWED | Posted: 25 September 2024 doi:10.20944/preprints202409.2002.v

			process (thickness reduced by 50%). The diameter of the neoplasm within the postoperative cicatrix decreased up to 50%		
		Systemic	Reduction of the diameter of the metastatic nidi in the liver by ~ 34%; elimination of some nidi in the lungs and reduction of their diameter by ~ 75%; reduction of the diameter of a paratracheal lymph node by ~ 36%; reduction of the diameter of paraaortic lymph nodes by ~ 50%	Stabilization of metastatic bone disease	Interstitial changes in the lungs
4	3	*Local*	Elimination of cutaneous nidi within the postoperative cicatrix and adjacent regions		Emergence of new intradermal nidi (neck and left shoulder)
		Systemic	Regression of pleurisy	Stabilization with respect to ascites, diffuse thickening of abdominal and retroperitoneal adipose tissue, pulmonary nidi and nidi in the osseous structures	Neutropenia
5	6	*Local*	Reduction of the diameter of tumor nidi in the breast by ~ 25%		Multiple intradermal deposits within the breast
		Systemic		Stabilization of pulmonary metastatic nidi	
6	2	*Local*			Local tumor progression, regional lymph node metastases, aggravation of edema. Emergence of intradermal deposits in the left

Preprints.org (www.preprints.org) | NOT PEER-REVIEWED | Posted: 25 September 2024 doi:10.20944/preprints202409.2002.v

					axillary region of the breast
		Systemic			Emergence of metastatic nidi in the lungs and pleura; Pleurisy. Emergence of metastatic nidi in the liver and spine
7	2	*Local*			Aggravation of breast edema and hyperemia, enlargement of lymph nodes
		Systemic			Leukopenia. Growth of metastatic nidi in the brain
8	2	*Local*	Reduction of hyperemia on the breast surface	Persistence of wound surface on the central breast region with necrotic and inflammatory foci and bleeding surface	
		Systemic			
9	4	*Local*	Reduction of tumor mass within the breast (area, ~ 35%), reduced swelling and exudation; cicatrization		Lymphedema in the right upper limb
		Systemic		Multiple focal pulmonary injury; focal neoplasm in the liver	Pleurisy. Anemia. Aggravation of the phenomenon of multiple organ system failure
10	3	*Local*	Decreased ulceration area size; Reduced hyperemia and size of skin metastasis		
		Systemic			
11	2	*Local*	Reduced skin metastasis		
		Systemic		Secondary changes in the lungs and bronchopulmonary lymph nodes; pleurisy	Anemia, acute intestinal obstruction – the course was interrupted

Preprints.org (www.preprints.org) | NOT PEER-REVIEWED | Posted: 25 September 2024 doi:10.20944/preprints202409.2002.v

12	5	*Local*	Reduced severity of breast edema, cicatrization of ulcers within the breast area
		Systemic	Positive dynamics for pleurisy (after administering the DNAmix into the pleural cavity)

Note: Local effect – tumor, peripheral lymph nodes, and skin metastasis.

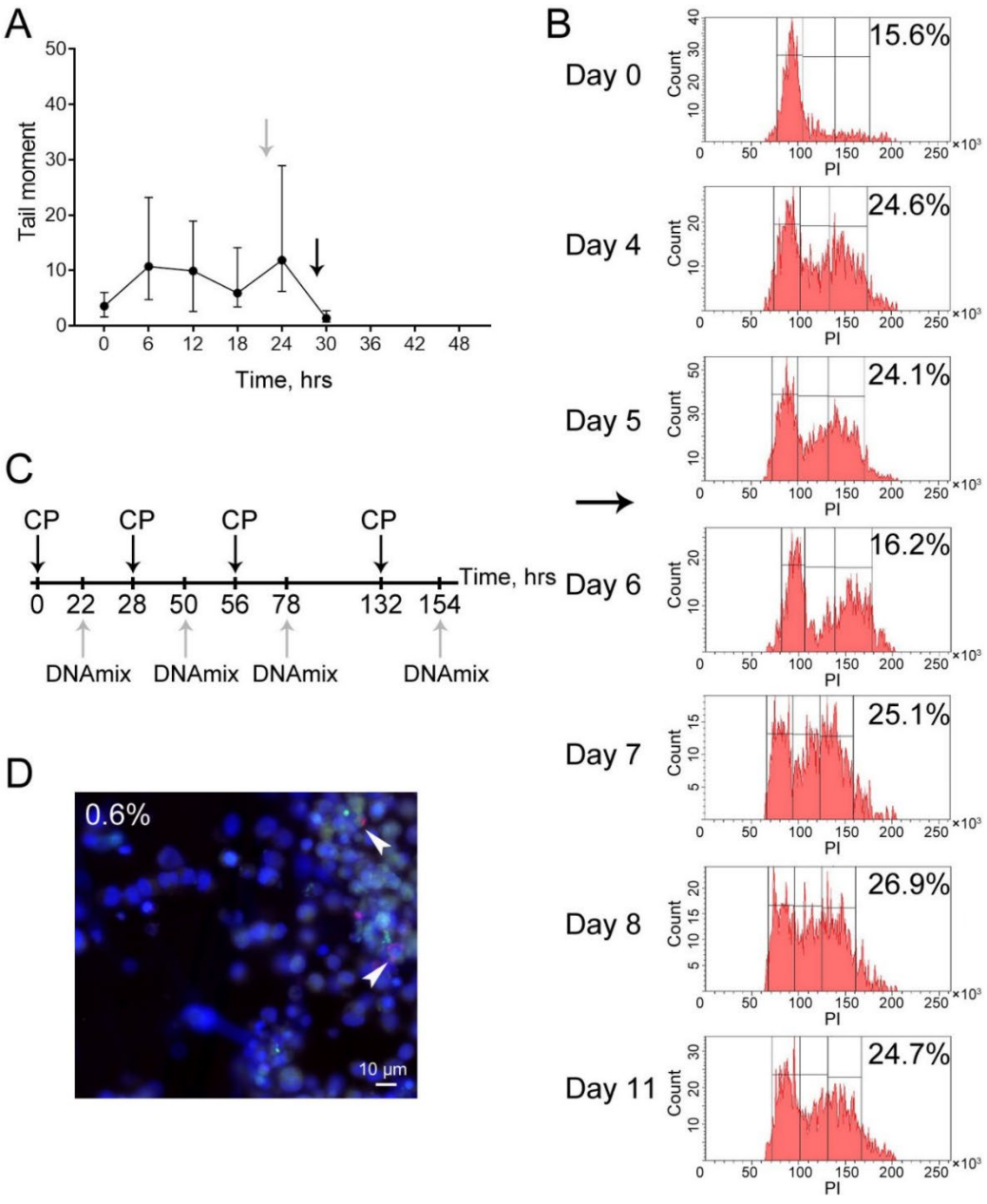

Figure 2. Patient 1. (A) DNA repair cycle in cancer cells. The medians and the 95% confidence interval for the tail moment in the comet assay are presented after different time intervals after the exposure of cells to 1 µg/mL mitomycin C are presented. The time of DNAmix administration determined for the future regimen is shown with a light gray arrow; the time of administration of a cross-linking cytostatic agent is indicated with a black arrow. (B) The cell cycle of cancer cells after three exposures

Preprints.org (www.preprints.org) | NOT PEER-REVIEWED | Posted: 25 September 2024 doi:10.20944/preprints202409.2002.v

to mitomycin C at an interval determined by analyzing the repair cycle; The cell cycle was quantified by flow cytometry according to propidium iodide fluorescence. The number of days after the initiation of treatment and the percentage of cells that undergo division are indicated. The black arrow shows the identified time of the fourth administration of the cytostatic cross-linking agent. (C) The resulting regimen of tumor treatment. The time of administration of CP and DNAmix is indicated. (D) Determining the number of TAMRA+ cancer stem cells. The percentage of cells is presented; arrows show examples of cancer cells internalizing the TAMRA-labeled probe.

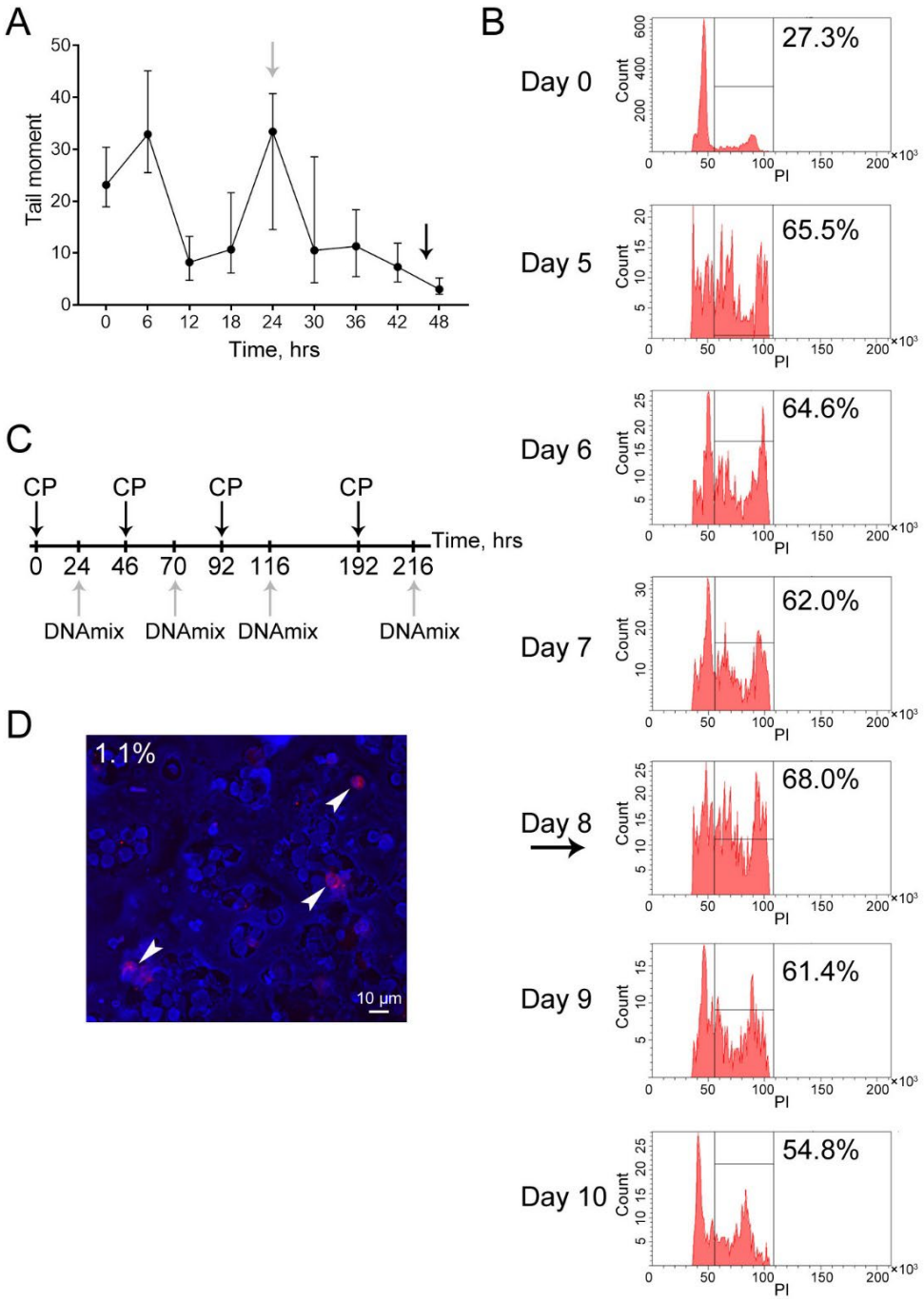

Figure 3. Patient 1-2, recurrence. (A) DNA repair cycle in cancer cells. The medians and the 95% confidence interval for the tail moment in the comet assay after different time intervals after the exposure of cells to 1 μg/mL mitomycin C are presented. The time of DNAmix administration determined for the future regimen is shown with a light gray arrow; the time of administration of a cross-linking cytostatic agent is indicated with a black arrow. (B) The cell cycle of cancer cells after three exposures to mitomycin C at an interval determined by analyzing the repair cycle; the cell cycle

Preprints.org (www.preprints.org) | NOT PEER-REVIEWED | Posted: 25 September 2024 doi:10.20944/preprints202409.2002.v

was quantified by flow cytometry according to propidium iodide fluorescence. The number of days after the initiation of treatment and the percentage of cells that undergo division are indicated. The black arrow shows the identified time of the fourth administration of the cytostatic cross-linking agent. (C) The resulting regimen of tumor treatment. The time of administering CP and DNAmix is indicated. (D) Determining the number of TAMRA+ cancer stem cells. The percentage of cells is presented; arrows show examples of cancer cells internalizing the TAMRA-labeled probe.

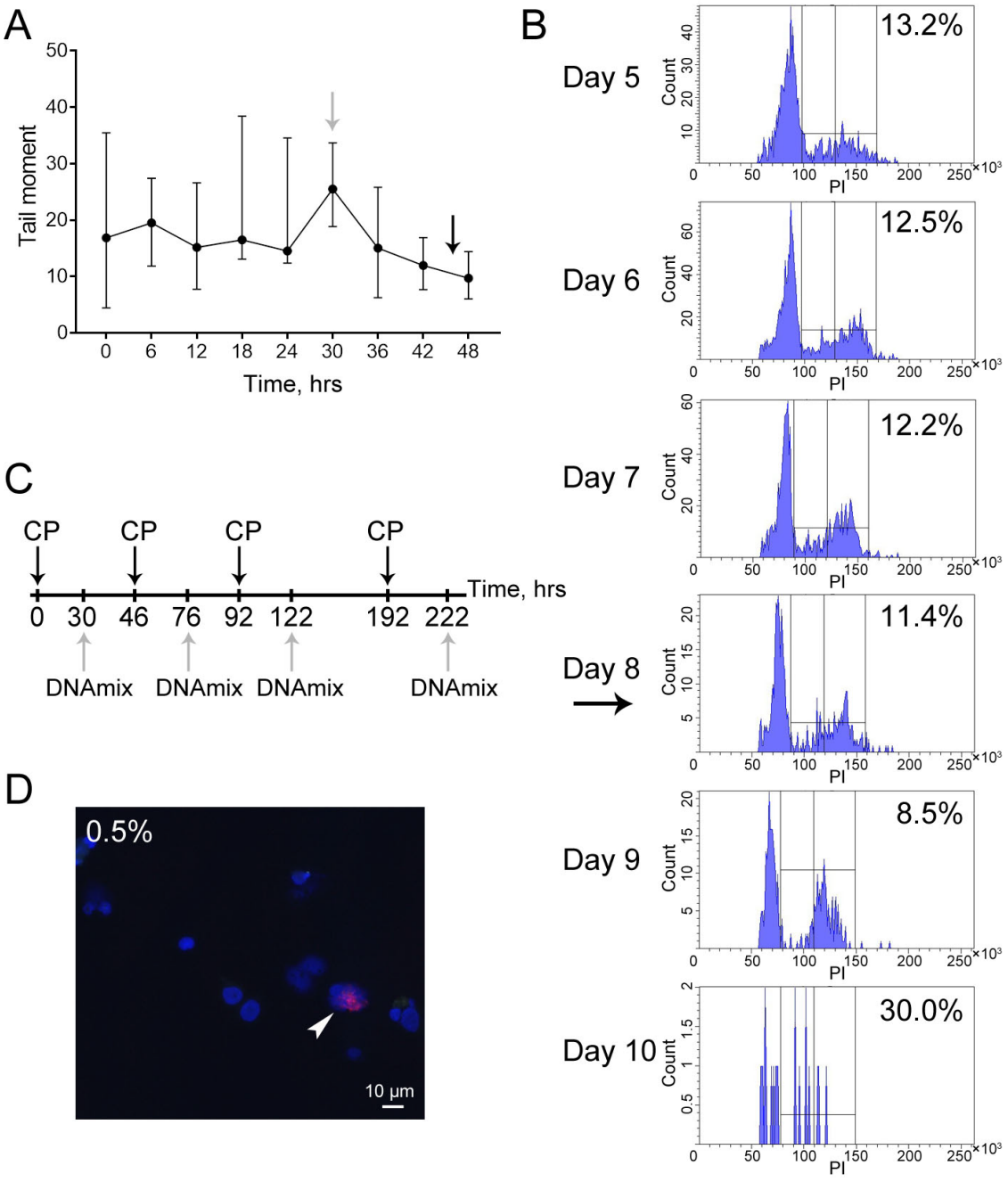

Figure 4. Patient 2. (A) DNA repair cycle in cancer cells. The medians and the 95% confidence interval for the tail moment in the comet assay after different time intervals after the exposure of cells to 1 µg/mL mitomycin C are presented. The time of DNAmix administration determined for the future regimen is shown with a light gray arrow; the time of administration of a cross-linking cytostatic agent is indicated with a black arrow. (B) The cell cycle of cancer cells after three exposures to mitomycin C at an interval determined by analyzing the repair cycle; the cell cycle was quantified by flow cytometry according to propidium iodide fluorescence. The number of days after the initiation of treatment and the percentage of cells that undergo division are indicated. The black arrow shows

Preprints.org (www.preprints.org) | NOT PEER-REVIEWED | Posted: 25 September 2024 doi:10.20944/preprints202409.2002.v

the identified time of the fourth administration of the cytostatic cross-linking agent. (C) The resulting regimen of tumor treatment. The time of administering CP and DNAmix is indicated. (D) Determining the number of TAMRA+ cancer stem cells. The percentage of cells is presented; arrows show examples of cancer cells internalizing the TAMRA-labeled probe.

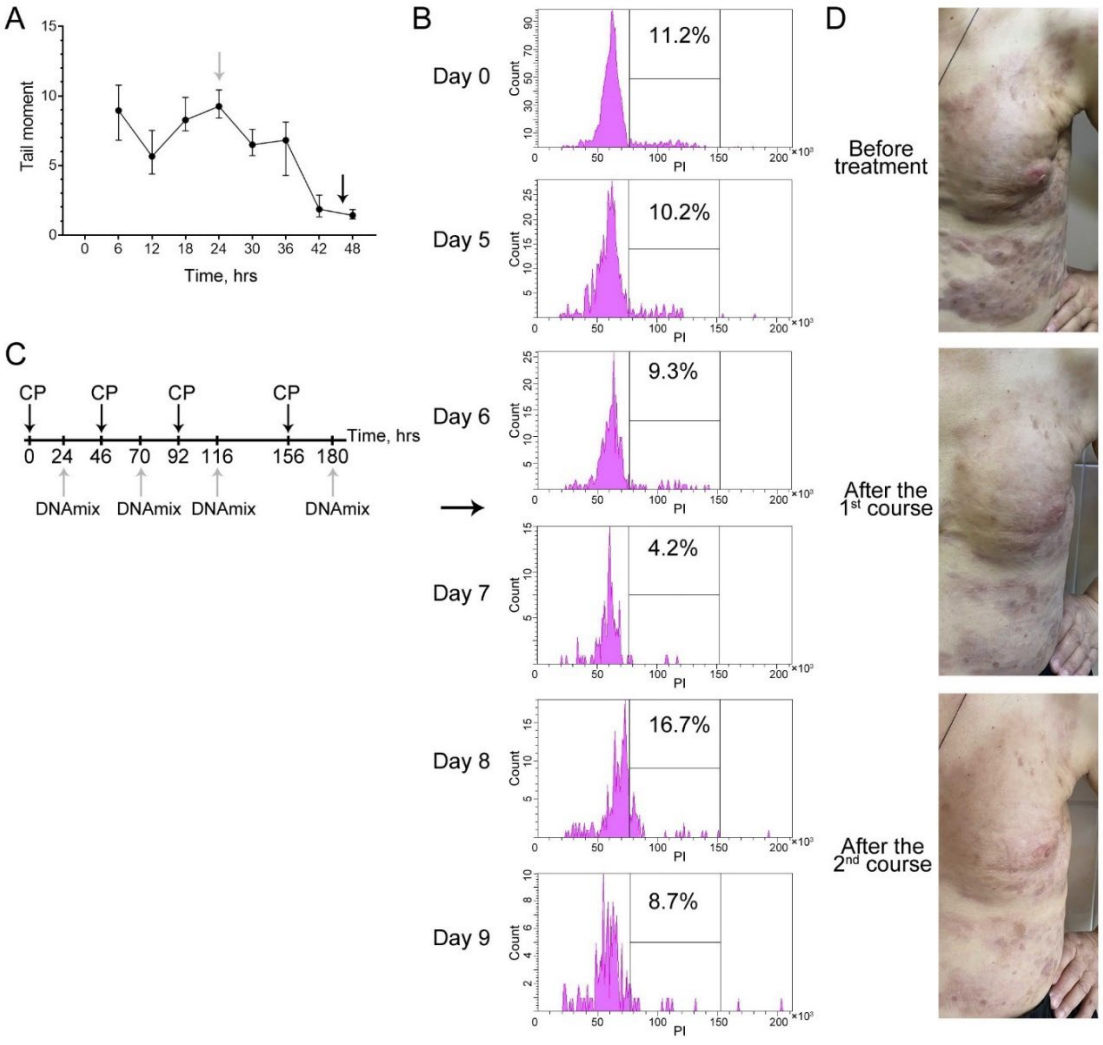

Figure 5. Patient 3. (A) DNA repair cycle in cancer cells. The medians and the 95% confidence interval for the tail moment in the comet assay after different time intervals after the exposure of cells to 1 μg/mL mitomycin C are presented. The time of DNAmix administration determined for the future regimen is shown with a light gray arrow; the time of administration of a cross-linking cytostatic agent is indicated with a black arrow. (B) The cell cycle of cancer cells after three exposures to mitomycin C at an interval determined by analyzing the repair cycle; the cell cycle was quantified by flow cytometry according to propidium iodide fluorescence. The number of days after the initiation of treatment and the percentage of cells that undergo division are indicated. The black arrow shows the identified time of the fourth administration of the cytostatic cross-linking agent. (C) The resulting regimen of tumor treatment. The time of administering CP and DNAmix is indicated. (D) Photographs of the main tumor nidi of the patient during therapy.

Preprints.org (www.preprints.org) | NOT PEER-REVIEWED | Posted: 25 September 2024 doi:10.20944/preprints202409.2002.v

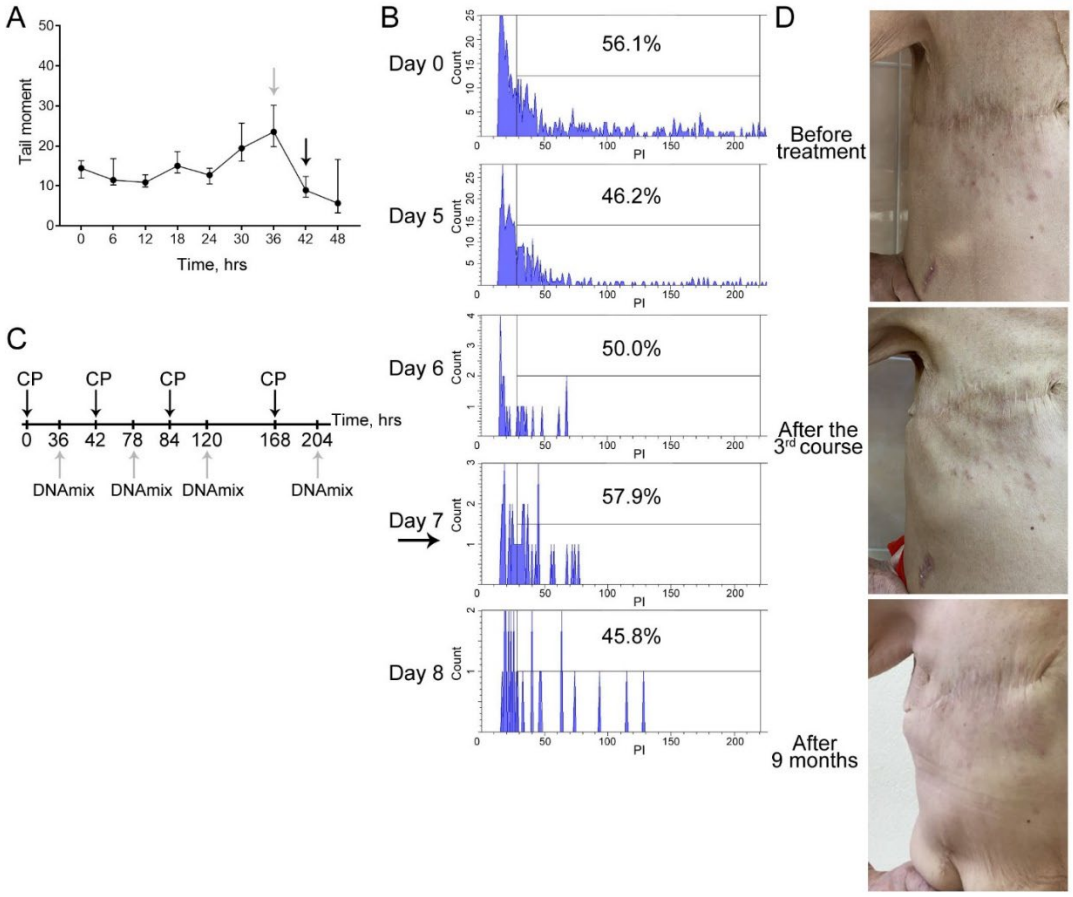

Figure 6. Patient 4. (A) DNA repair cycle in cancer cells. The medians and the 95% confidence interval for the tail moment in the comet assay after different time intervals after the exposure of cells to 1 μg/mL mitomycin C are presented. The time of DNAmix administration determined for the future regimen is shown with a light gray arrow; the time of administration of a cross-linking cytostatic agent is indicated with a black arrow. (B) The cell cycle of cancer cells after three exposures to mitomycin C at an interval determined by analyzing the repair cycle; the cell cycle was quantified by flow cytometry according to propidium iodide fluorescence. The number of days after the initiation of treatment and the percentage of cells that undergo division are indicated. The black arrow shows the identified time of the fourth administration of the cytostatic cross-linking agent. (C) The resulting regimen of tumor treatment. The time of administering CP and DNAmix is indicated. (D) Photographs of the main tumor nidi of the patient during therapy.

Preprints.org (www.preprints.org) | NOT PEER-REVIEWED | Posted: 25 September 2024 doi:10.20944/preprints202409.2002.v

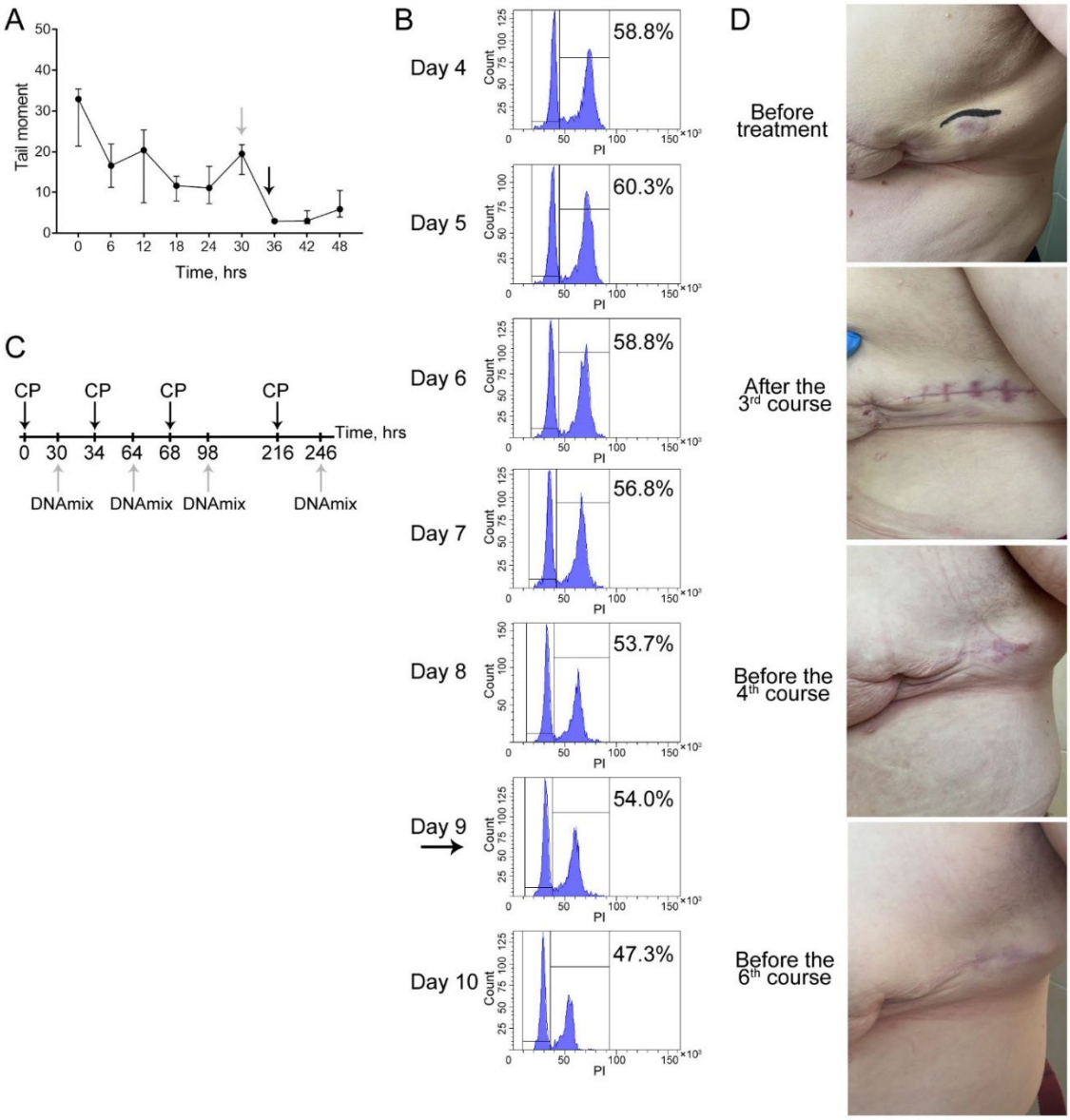

Figure 7. Patient 5. (A) DNA repair cycle in cancer cells. The medians and the 95% confidence interval for the tail moment in the comet assay after different time intervals after the exposure of cells to 1 μg/mL mitomycin C are presented. The time of DNAmix administration determined for the future regimen is shown with a light gray arrow; the time of administration of a cross-linking cytostatic agent is indicated with a black arrow. (B) The cell cycle of cancer cells after three exposures to mitomycin C at an interval determined by analyzing the repair cycle; the cell cycle was quantified by flow cytometry according to propidium iodide fluorescence. The number of days after the initiation of treatment and the percentage of cells that undergo division are indicated. The black arrow shows the identified time of the fourth administration of the cytostatic cross-linking agent. (C) The resulting regimen of tumor treatment. The time of administering CP and DNAmix is indicated. (D) Photographs of the main tumor nidi of the patient during therapy.

Preprints.org (www.preprints.org) | NOT PEER-REVIEWED | Posted: 25 September 2024 doi:10.20944/preprints202409.2002.v

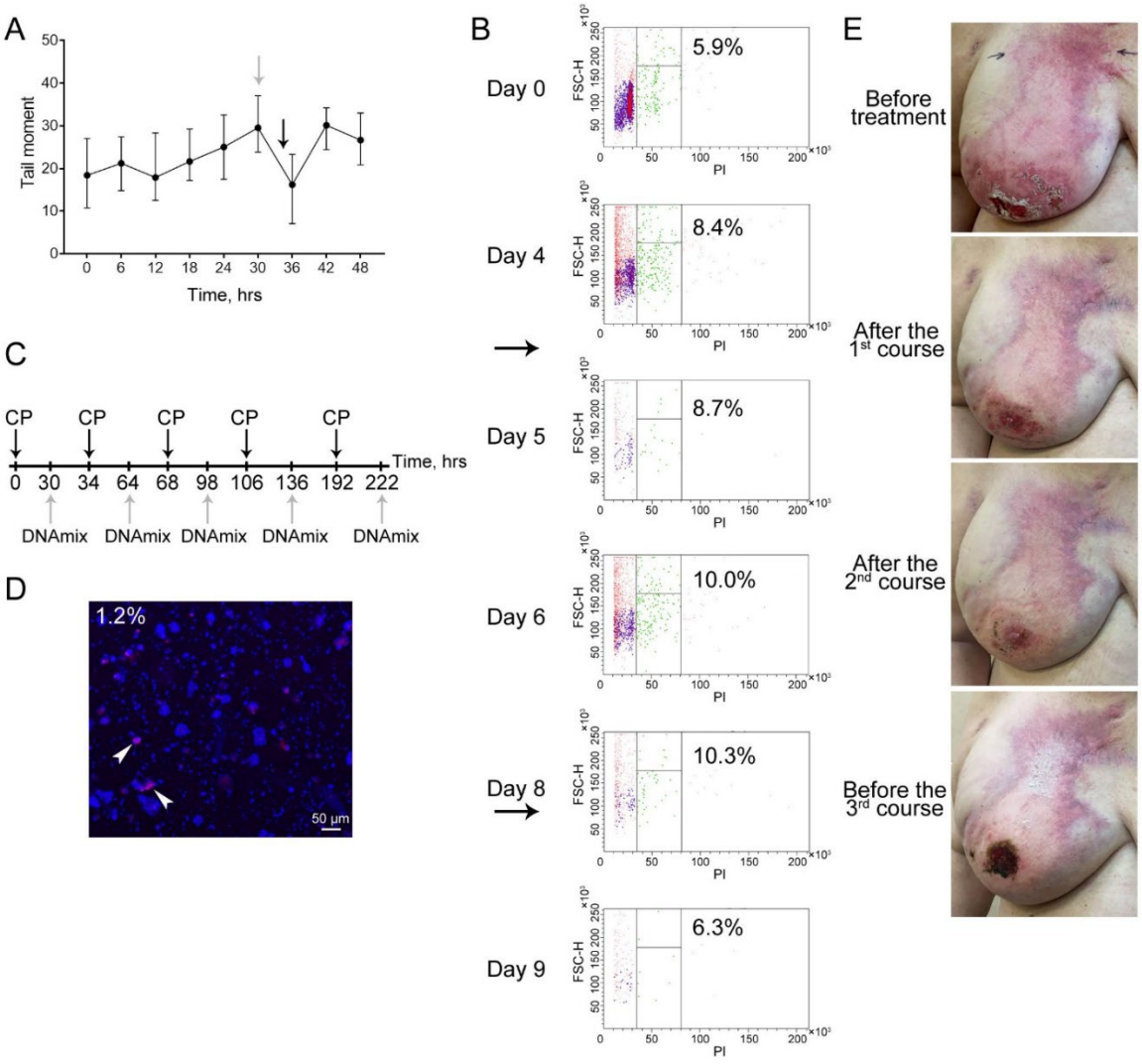

Figure 8. Patient 6. (A) DNA repair cycle in cancer cells. The medians and the 95% confidence interval for the tail moment in the comet assay after different time intervals after the exposure of cells to 1 μg/mL mitomycin C are presented. The time of DNAmix administration determined for the future regimen is shown with a light gray arrow; the time of administration of a cross-linking cytostatic agent is indicated with a black arrow. (B) The cell cycle of cancer cells after three exposures to mitomycin C at an interval determined by analyzing the repair cycle; the cell cycle was quantified by flow cytometry according to propidium iodide fluorescence. The number of days after the initiation of treatment and the percentage of cells that undergo division are indicated. The black arrow shows the identified time of the fourth administration of the cytostatic cross-linking agent. (C) The resulting regimen of tumor treatment. The time of administering CP and DNAmix is indicated. (D) Determining the number of TAMRA+ cancer stem cells. The percentage of cells is presented; arrows show examples of cancer cells internalizing the TAMRA-labeled probe. (E) Photographs of the main tumor nidi of the patient during therapy.

Preprints.org (www.preprints.org) | NOT PEER-REVIEWED | Posted: 25 September 2024 doi:10.20944/preprints202409.2002.v

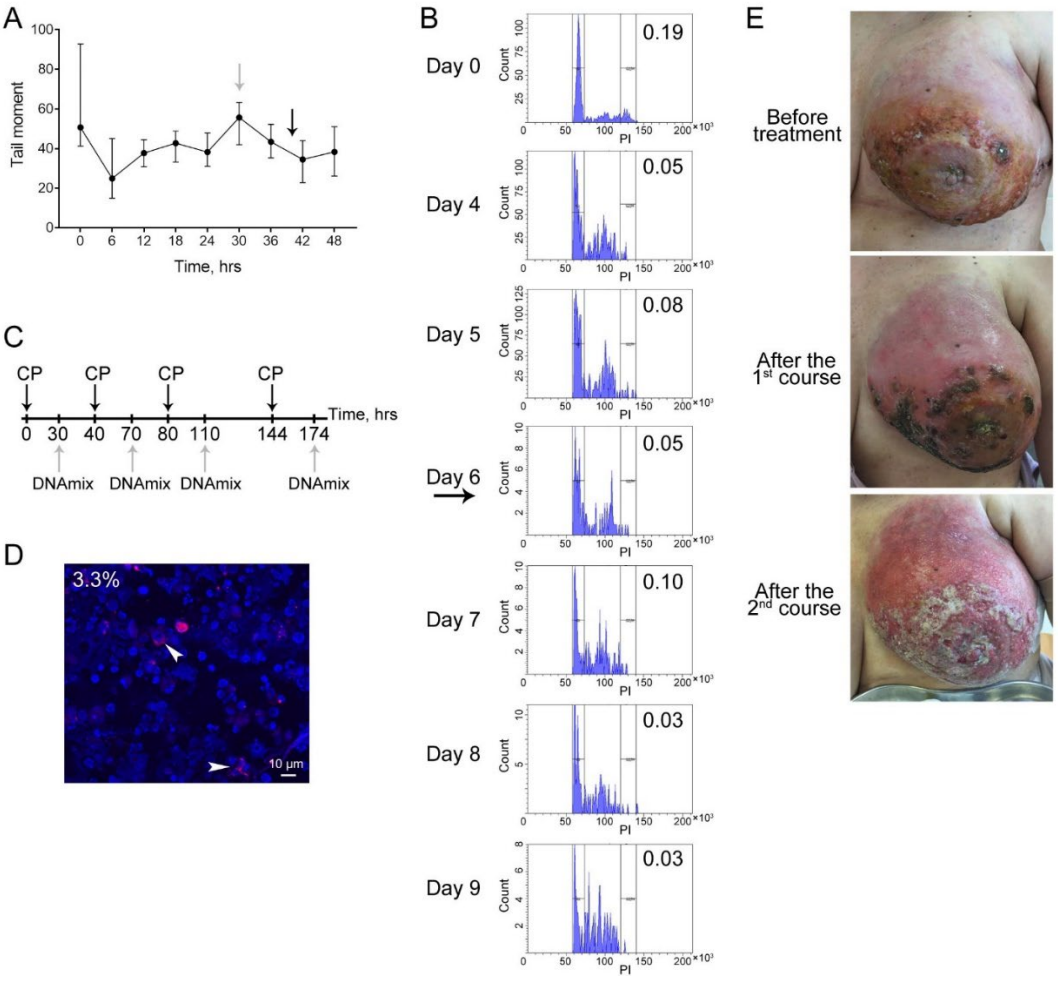

Figure 9. Patient 7. (A) DNA repair cycle in cancer cells. The medians and the 95% confidence interval for the tail moment in the comet assay after different time intervals after the exposure of cells to 1 μg/mL mitomycin C are presented. The time of DNAmix administration determined for the future regimen is shown with a light gray arrow; the time of administration of a cross-linking cytostatic agent is indicated with a black arrow. (B) The cell cycle of cancer cells after three exposures to mitomycin C at an interval determined by analyzing the repair cycle; the cell cycle was quantified by flow cytometry according to propidium iodide fluorescence. The number of days after the initiation of treatment and the ratio between the percentage of cells undergoing division in the G2/M phase and the percentage of cells in the G1 phase are indicated. The black arrow shows the identified time of the fourth administration of the cytostatic cross-linking agent. (C) The resulting regimen of tumor treatment. The time of administering CP and DNAmix is indicated. (D) Determining the number of TAMRA+ cancer stem cells. The percentage of cells is presented; arrows show examples of cancer cells internalizing the TAMRA-labeled probe. (E) Photographs of the main tumor nidi of the patient during therapy.

Preprints.org (www.preprints.org) | NOT PEER-REVIEWED | Posted: 25 September 2024 doi:10.20944/preprints202409.2002.v

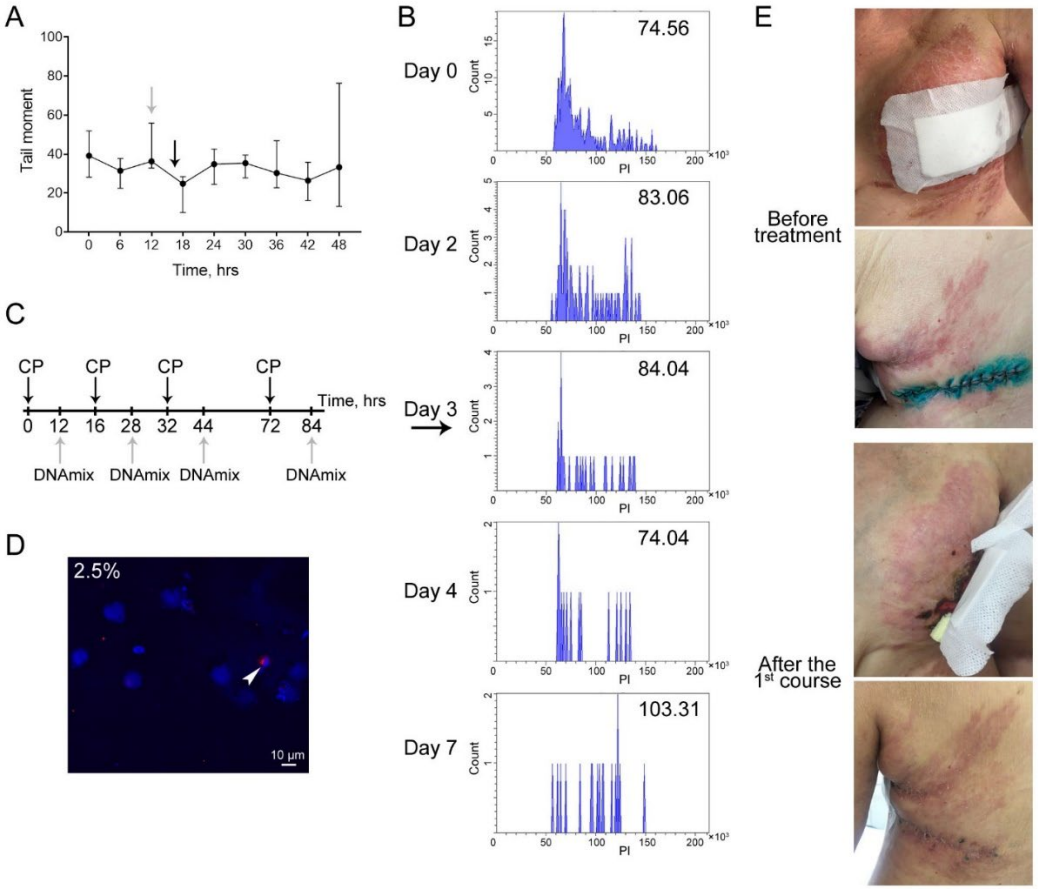

Figure 10. Patient 8. (A) DNA repair cycle in cancer cells. The medians and the 95% confidence interval for the tail moment in the comet assay after different time intervals after the exposure of cells to 1 µg/mL mitomycin C are presented. The time of DNAmix administration determined for the future regimen is shown with a light gray arrow; the time of administration of a cross-linking cytostatic agent is indicated with a black arrow. (B) The cell cycle of cancer cells after three exposures to mitomycin C at an interval determined by analyzing the repair cycle; the cell cycle was quantified by flow cytometry according to propidium iodide fluorescence. The number of days after the initiation of treatment and the median percentage of cells exhibiting propidium iodide fluorescence are indicated. The black arrow shows the identified time of the fourth administration of the cytostatic cross-linking agent. (C) The resulting regimen of tumor treatment. The time of administering CP and DNAmix is indicated. (D) Determining the number of TAMRA+ cancer stem cells. The percentage of cells is presented; arrows show examples of cancer cells internalizing the TAMRA-labeled probe. (E) Photographs of the main tumor nidi of the patient during therapy.

Preprints.org (www.preprints.org) | NOT PEER-REVIEWED | Posted: 25 September 2024 doi:10.20944/preprints202409.2002.v

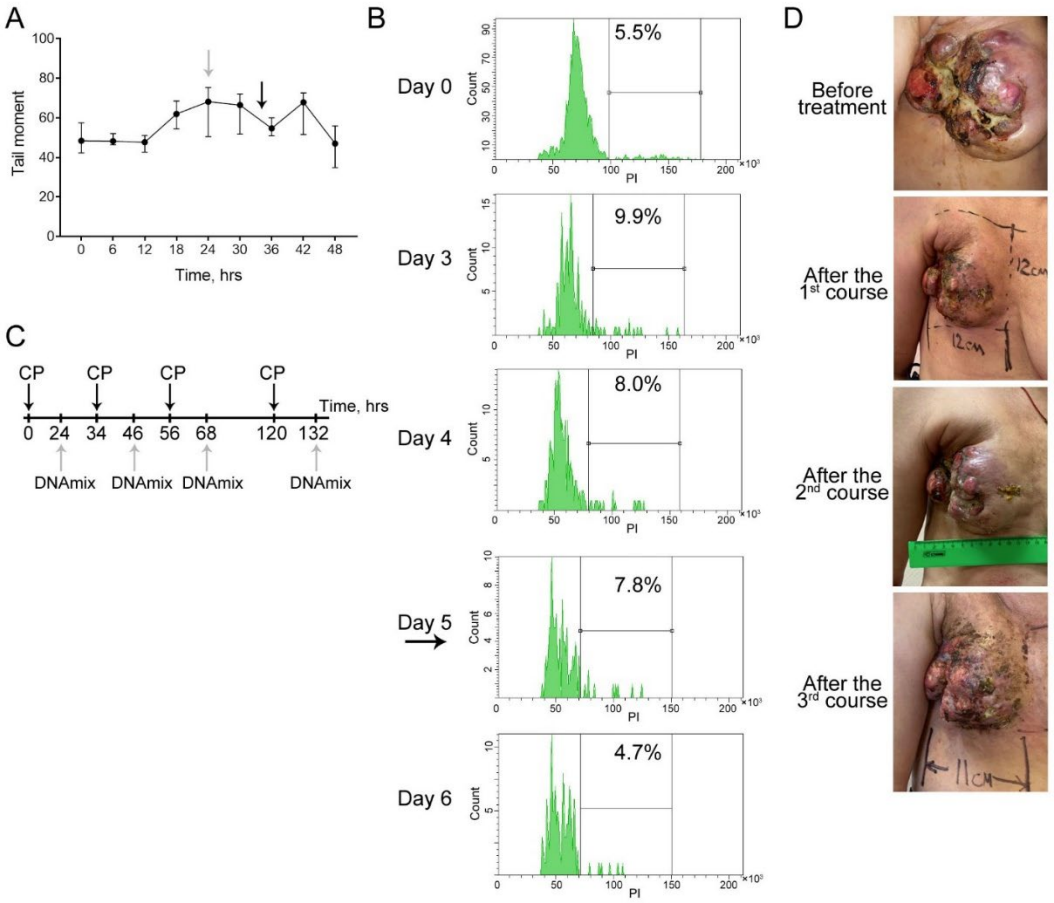

Figure 11. Patient 9. (A) DNA repair cycle in cancer cells. The medians and the 95% confidence interval for the tail moment in the comet assay after different time intervals after the exposure of cells to 1 μg/mL mitomycin C are presented. The time of DNAmix administration determined for the future regimen is shown with a light gray arrow; the time of administration of a cross-linking cytostatic agent is indicated with a black arrow. (B) The cell cycle of cancer cells after three exposures to mitomycin C at an interval determined by analyzing the repair cycle; the cell cycle was quantified by flow cytometry according to propidium iodide fluorescence. The number of days after the initiation of treatment and the percentage of cells that undergo division are indicated. The black arrow shows the identified time of the fourth administration of the cytostatic cross-linking agent. (C) The resulting regimen of tumor treatment. The time of administering CP and DNAmix is indicated. (D) Photographs of the main tumor nidi of the patient during therapy.

Preprints.org (www.preprints.org) | NOT PEER-REVIEWED | Posted: 25 September 2024 doi:10.20944/preprints202409.2002.v

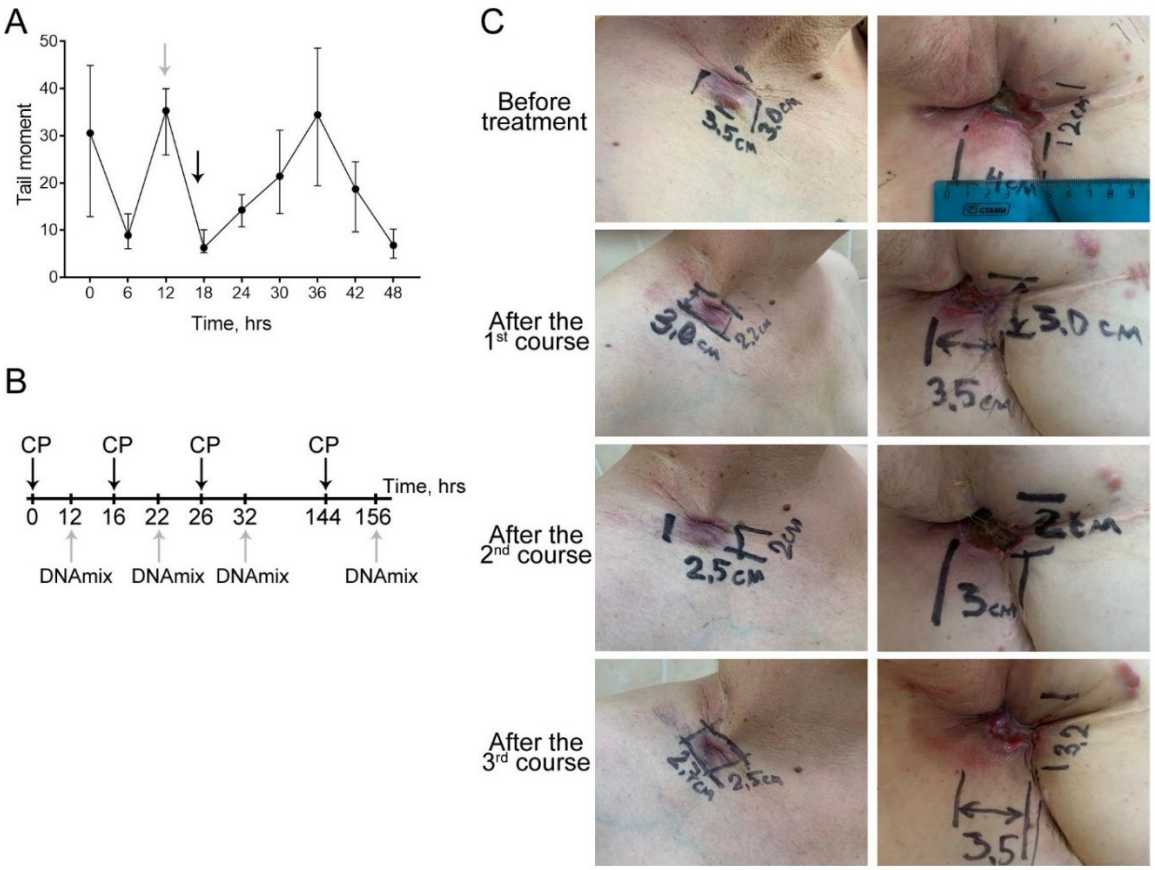

Figure 12. Patient 10. (A) DNA repair cycle in cancer cells. The medians and the 95% confidence interval for the tail moment in the comet assay after different time intervals after the exposure of cells to 1 μg/mL mitomycin C are presented. The time of DNAmix administration determined for the future regimen is shown with a light gray arrow; the time of administration of a cross-linking cytostatic agent is indicated with a black arrow. (B) The resulting regimen of tumor treatment. The time of administering CP and DNAmix is indicated. (C) Photographs of the main tumor nidi of the patient during therapy.

Preprints.org (www.preprints.org) | NOT PEER-REVIEWED | Posted: 25 September 2024 doi:10.20944/preprints202409.2002.v

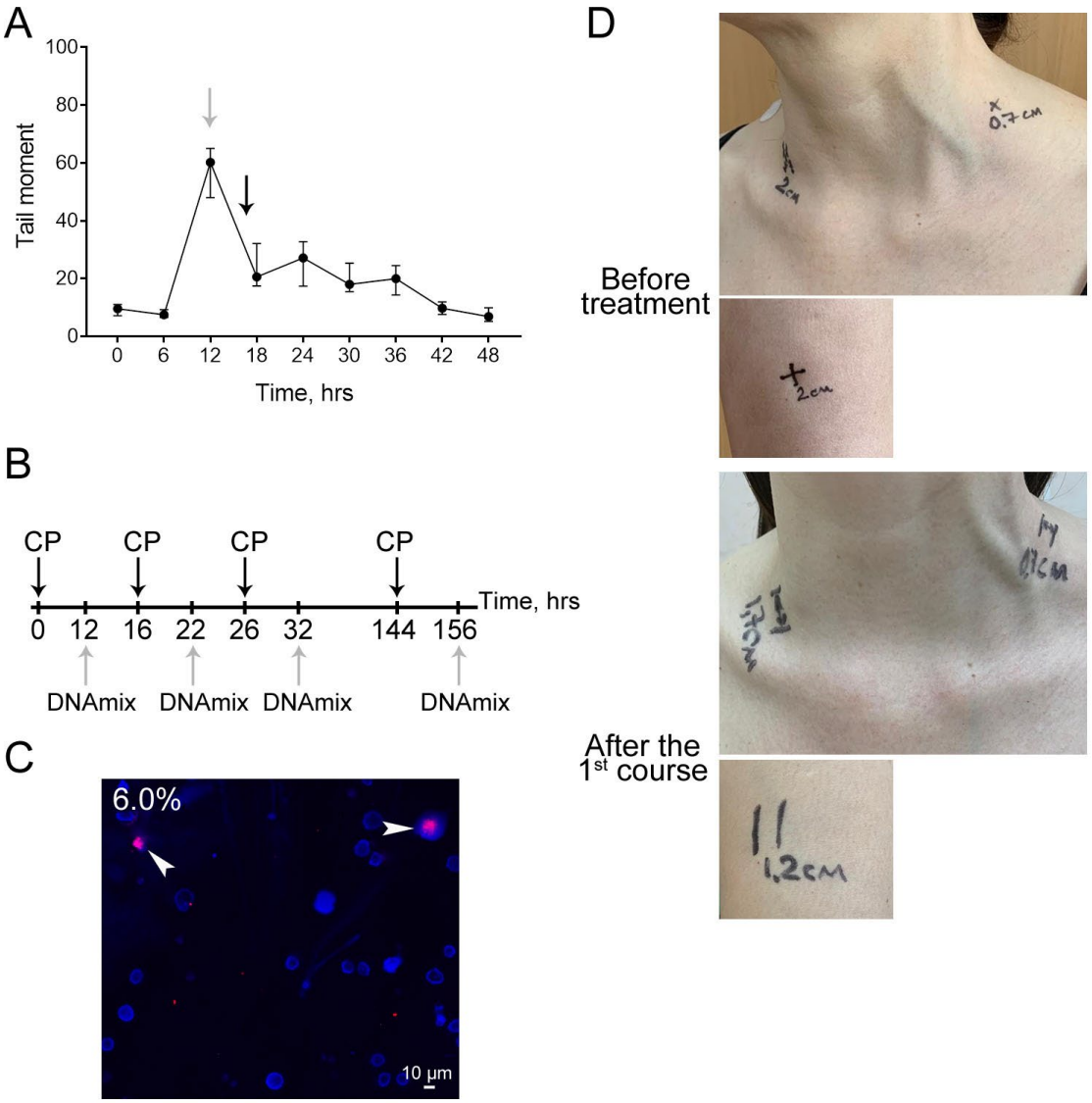

Figure 13. Patient 11. (A) DNA repair cycle in cancer cells. The medians and the 95% confidence interval for the tail moment in the comet assay after different time intervals after the exposure of cells to 1 μg/mL mitomycin C are presented. The time of DNAmix administration determined for the future regimen is shown with a light gray arrow; the time of administration of a cross-linking cytostatic agent is indicated with a black arrow. (B) The resulting regimen of tumor treatment. The time of administering CP and DNAmix is indicated. (C) Determining the number of TAMRA+ cancer stem cells. The percentage of cells is presented; arrows show examples of cancer cells internalizing the TAMRA-labeled probe. (D) Photographs of the main tumor nidi of the patient during therapy.

Preprints.org (www.preprints.org) | NOT PEER-REVIEWED | Posted: 25 September 2024 doi:10.20944/preprints202409.2002.v

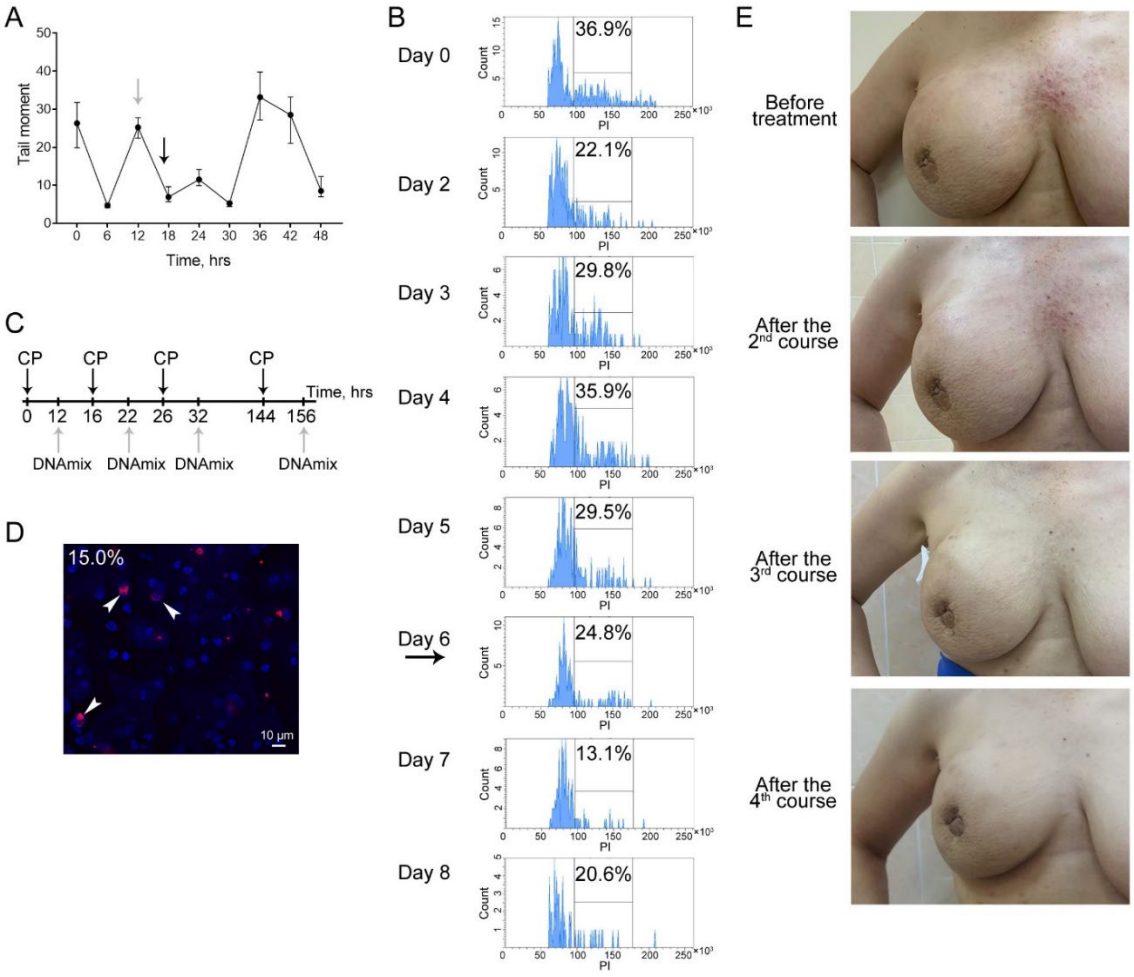

Figure 14. Patient 12. (A) DNA repair cycle in cancer cells. The medians and the 95% confidence interval for the tail moment in the comet assay after different time intervals after the exposure of cells to 1 μg/mL mitomycin C are presented. The time of DNAmix administration determined for the future regimen is shown with a light gray arrow; the time of administration of a cross-linking cytostatic agent is indicated with a black arrow. (B) The cell cycle of cancer cells after three exposures to mitomycin C at an interval determined by analyzing the repair cycle; the cell cycle was quantified by flow cytometry according to propidium iodide fluorescence. The number of days after the initiation of treatment and the median percentage of cells exhibiting propidium iodide fluorescence are indicated. The black arrow shows the identified time of the fourth administration of the cytostatic cross-linking agent. (C) The resulting regimen of tumor treatment. The time of administering CP and DNAmix is indicated. (D) Determining the number of TAMRA+ cancer stem cells. The percentage of cells is presented; arrows show examples of cancer cells internalizing the TAMRA-labeled probe. (E) Photographs of the main tumor nidi of the patient during therapy.

3.2.2. Assessment of the Survival Time for Non-Survivors in the Experimental Cohort vs. Historical Control

The survival time of patients after palliative status has been given is one of the socially significant criteria in evaluating the efficacy of treating patients with conditions selected to conduct the present study. The evaluation of this parameter is presented in Supplementary Material 4. The parameters of the experimental group and the historical control are compared.

A comparative analysis of survival time demonstrates that *Karanahan* technology significantly increases the time interval before patient death (Figure 15).

Preprints.org (www.preprints.org) | NOT PEER-REVIEWED | Posted: 25 September 2024 doi:10.20944/preprints202409.2002.v

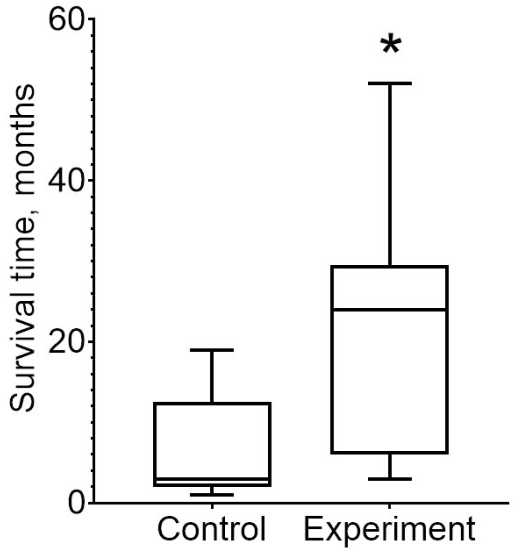

Figure 15. Comparative analysis of the survival time of patients in the control group and in the experimental group (receiving therapy using *Karanahan* technology). * – statistically significant differences, $p < 0.05$, Mann–Whitney U test.

3.2.3. Quality of Life Assessment

Patients' feedback on quality of life and tolerability of treatment was collected throughout the study. The resulting data are summarized in Table 3.

The quality of life score was significantly increased for three patients (Nos. 9, 10, and 11), being consistent with the objective indicators after therapy using *Karanahan* technology. A significant worsening of well-being was observed for a single patient (no. 6), which was consistent with the fact that local tumor progression was detected and new metastatic foci emerged in this patient.

Table 3. Changes in patient quality of life during therapy (score) according to the EORTC QLQ-C30 questionnaires (version 3.0) filled out by patients.

Patient No.	Before the 1st course	Before the 3rd course
1-2	59	53
5	45	41
6	105	61
7	91	95
8	84	70
9	53	90
10	50	71
11	51	81
12	75	72

3.2.4. Tumor Response According to the RECIST System

The clinically manifested tumor response observed after therapy with *Karanahan* technology was analyzed. The results of the analysis were brought in line with the criteria of RECIST 1.1 and are summarized in Table 4.

Complete or partial tumor response to *Karanahan* technology therapy or disease stabilization was observed in eight patients; disease progression occurred in two patients (no. 6 and no. 7). Another two patients (no. 2 and no. 4) had a positive local response, but disease progression (emergence of new metastatic foci) was also observed.

Preprints.org (www.preprints.org) | NOT PEER-REVIEWED | Posted: 25 September 2024 doi:10.20944/preprints202409.2002.v

Table 4. Tumor response according to the RECIST 1.1 system.

Patient No.	Complete response (CR)	Partial response (PR)	Stabilization of disease (SD)	Progression of disease (PD)
1	●			
1-2			●	
2		● (breast)		● (liver, osseous structures)
3		●		
4			● (locally)	● (liver, osseous structures)
5			●	
6				●
7				●
8			●	
9		●		
10			●	
11			●	
12		●		

Note: Compete response (CR) – elimination of all tumor nidi. Partial response (PR) – the sum of maximum diameters of each nidus is reduced by > 30%. Stabilization of disease (SD) – the sum of maximum diameters of each nidus is reduced by 20–30%. Neither partial resorption nor progression is observed. Progression of disease (PD) – the sum of maximum diameters of each nidus increases by > 20% or new tumor nidi appear.

3.2.5. Quantification of Regulatory T Cells and CD8 Populations in Peripheral Blood

Determining the response of the immune system to the conducted therapy is a required analysis. We selected two parameters that provide a general view of the antitumor immunity level (Figure 16, Supplementary Material 5). An analysis of changes in the number of regulatory T cells allows one to draw a conclusion about the self-defense potential of the tumor. An analysis of changes in the number and cytotoxic activity of cytotoxic T cells gives grounds for drawing a conclusion about antitumor immune responses.

The degranulation of cytotoxic lymphocytes is the key indicator of the maturity and cytolytic activity of T cells, which is associated, among other factors, with their effect on tumor cells through specific antigens. Lysosomal granules containing cytolytic proteins are present in T cells. In differentiated CD8+ T cells, TLR-mediated stimulation causes degranulation (ie, release of the contents of the lytic granules). Meanwhile, a CD107a molecule, a component of lytic granules, is placed on the surface of the T cell, which is used as a functional marker of cytotoxic lymphocytes. The externalization of CD107a on the surface of CD8 T cells was evaluated in the degranulation test.

The conducted analysis shows that the suppressive effect of the tumor on the body after therapy with *Karanahan* technology is not fundamentally changed, while the activity of the adaptive antitumor immune response increases significantly.

Preprints.org (www.preprints.org) | NOT PEER-REVIEWED | Posted: 25 September 2024 doi:10.20944/preprints202409.2002.v

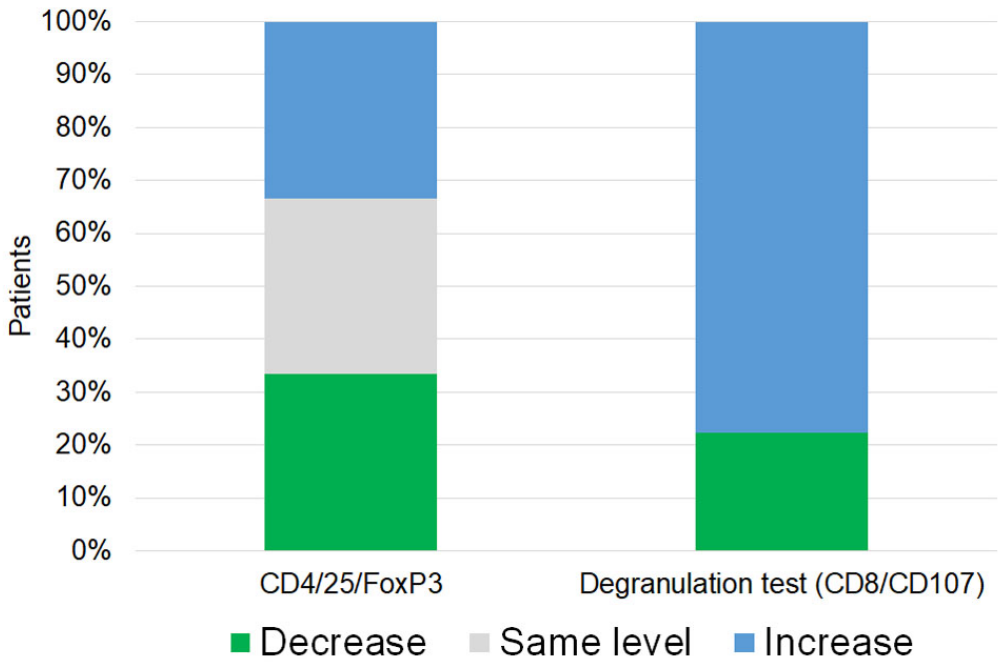

Figure 16. Assessment of changes in regulatory T cell and CD8 populations. The percentages of patients who had an increased, the same or reduced number of CD4/25/FoxP3 cells and degranulation test values are presented.

4. Discussion

In our studies conducted over the past five years, we have discovered and performed cell-level characterization of a general biological phenomenon that has remained unknown until recently: the ability of poorly differentiated cells, including cancer stem cells, to internalize fragments of double-stranded extracellular DNA via a natural internalization mechanism without employing the transfection procedure. A unique universal marker of stem cells of different genesis, including cancer stem cells, was fabricated using a fluorochrome-labeled DNA probe.

It was found simultaneously that double-stranded DNA fragments internalized in the cellular space of cancer stem cells during repair of CP-induced interstrand crosslinks interfere with the DNA repair process in such a way that they completely eradicate the malignant potential of the grafted tumor. The elimination of cancer stem cells from the mass of engrafted cancer cells was the key factor in the loss of tumorigenic properties by the graft [41–44].

Therefore, we have experimentally identified two components that underlie a fundamentally new strategy to treat malignant neoplasms. Furthermore, the general biological nature of the discovery allows us to focus on novel ways to influence stem cells and develop novel technologies for manipulating cellular genetics and properties.

In this pilot project, we have challenged ourselves to evaluate the potential favorable effects of the novel technology in real clinical practice for the breast cancer model in cases of stage IV cancer. Breast cancer was chosen as a model disease due to its high prevalence as well as the social significance of successful treatment of this disease. Being fully aware of the legal and procedural challenges associated with the novel therapy, we focused on palliative patients with advanced stage IV breast cancer. The possibility of observing favorable clinical effects in such advanced cancer cases could justify the search for clinical regimens that allow the elimination of tumor nidus and bring patients to remission even at such an advanced stage of the disease.

An analysis of the effect of *Karanahan* technology on stage IV breast cancer progression revealed that (1) the survival time for analyzed patients was significantly increased, thus undoubtedly being a socially significant outcome, and (2) the positive dynamics within the most pronounced tumor nidi was observed locally, at the DNAmix injection sites.

Preprints.org (www.preprints.org) | NOT PEER-REVIEWED | Posted: 25 September 2024 doi:10.20944/preprints202409.2002.v

Patient 2 had tumor nidi on both breasts. The tumor in the right breast was palpable; the tumor in the left breast occupied the entire gland volume and was a very dense conglomerate. After two cycles of therapy, the tumor in the right breast was no longer palpable. The affected tissue was rejected as necrotic fistulas. The tumor in the left breast became significantly smaller and soft. In other words, the primary nidus had undergone a positive transformation.

In the case of patient 9, after three consecutive treatments using the new technology, the necrotizing tumor shrank and became smaller; tissue decay almost stopped; the edges of the wounds of the surface were epithelialized; and the ichorous odor subsided. Tumor cells could not be isolated from the tissue sample after three therapy cycles, and the nidus appeared to have transformed into a fibrous stroma.

As mentioned above, although the patients' survival time had increased significantly, a pronounced systemic response and a reduction in the size of all tumor nidi in the liver, bones, and skin were not achieved in a particular situation. We believe that the insufficiently pronounced systemic response is caused by two factors. First, it is the inadequate estimation of the biological clock of the DNA repair cycle and the cell cycle of tumor cells, which is related to the state of the original cellular material and will be difficult to correct. Second, there is the problem of delivering the required drug doses to the tumor nidus at the right time and the loss of effective dose associated with it. Thus, phosphoramide mustard, the CP metabolite that is formed in the liver, either does not reach the target zones due to poor blood supply (for skin and bone metastases) or is broken down as it passes through systemic circulation (for liver metastasis), and only a manifold reduced dose of the cross-linking agent is delivered to the liver.

When injected intratumorally at the original dose (1 mg per therapy point), DNAmix has an impact only on a small portion of the affected tissue. In this case, only some cancer stem cells are exposed to the eradication effect of medications.

The proliferation of dormant metastases can be activated when the therapeutic effect of the drugs is incomplete (i.e., the cytostatic agent has induced cross-links, but the DNAmix failed to reach this nidus at the proper time). The interstrand crosslinks in cancer stem cells will be repaired, the cells will not acquire apoptotic status, and so-called clonal selection will occur [45,46]. This situation will result in additional tumor progression.

Therefore, we inferred that it is reasonable to increase the drug dose (to a dose close to the one used in mouse experiments) and optimize the regimen of DNAmix delivery. The dose of DNAmix was increased to 12 mg in 12 mL of saline. Additionally, a decision was made that instead of trying systemic administration of DNAmix, injections should be made into lymph depots within inguinal and axillary lymph node clusters, as well as at a distance of 5 to 7 cm to the right of the umbilicus (paraumbilically); injections in the most prominent local tumor nidi are prioritized. It is anticipated that DNAmix is injected into lymph depot areas, therapeutic DNA fragments will spread along lymph flow in an ascending direction, embracing the target areas of metastatic tumor nidi. When administered into the bloodstream, DNA is immediately degraded and loses its therapeutic effect [47].

The adjusted regimen was used, starting September 2023, for patient 12 with carcinomatous pleurisy, and an immediate favorable clinical response was achieved. The standard regimen was used for this patient during the first three courses: 1 mg of DNAmix was administered locally (intratumorally); injections were made into the most prominent tumor areas. Starting with the fourth therapy course, we used the new therapeutic regimen when high-dose DNAmix was injected into the lymph depot areas and the pleural cavity. Before switching to a different therapy regimen, the patient suffered the most from dyspnea caused by the accumulation of fluid in the pleural cavities and the need to drain the fluid by puncture. After starting the new drug regimen, the severity of the patient's dyspnea decreased, making frequent invasive procedures unnecessary and having a beneficial impact on her quality of life.

We demonstrated that *Karanahan* technology also activates the adaptive antitumor immune response, which undoubtedly favorably affects treatment.

5. Conclusions

Preprints.org (www.preprints.org) | NOT PEER-REVIEWED | Posted: 25 September 2024 doi:10.20944/preprints202409.2002.v

On the basis of these findings, it is fair to say that comprehensive application of the technology, when the DNA preparation reaches all tumor nidi, changes the tumor status and makes it operable. Furthermore, in the case of positive dynamics, it is possible to return to medications that had to be ceased because of ineffectiveness due to generalization and terminal progression of the neoplasm.

By continuing pilot clinical trials, where parameters can be varied throughout therapy, one can identify the regimen for achieving complete remission in patients with stage IV breast cancer, as has been demonstrated in numerous mouse models [31,33,34,36].

6. Patents

The Method for treating advanced breast cancer in the terminal stage of progression has been patented (priority No. 2024106957 dated Marth 14, 2024).

Supplementary Materials: The following supporting information can be downloaded at the website of this paper posted on Preprints.org. Supplementary Material 1. The procedure for intratumoral injection of DNA preparation. Supplementary Material 2. Modifications made to the protocol of therapy using Karanahan technology. Supplementary Material 3. Description of clinical manifestations during application of Karanahan. Supplementary Material 4. Survival time of patients. Supplementary Material 5. Quantification of regulatory T cells and CD8 populations in peripheral blood.

Author Contributions: Conceptualization, S.V.S. and S.S.B.; methodology, V.S.R. and E.I.V.; validation, S.S.K. and E.V.L.; formal analysis, A.S.P. and E.V.D.; investigation, V.A.M., V.S.R., G.S.R., S.G.O., Y.R.E., O.Y.L.; data curation, V.A.M.; writing—original draft preparation, V.A.M., A.S.P. and S.S.B.; writing—review and editing, A.S.P. and S.S.B.; visualization, A.S.P.; supervision, A.A.O. and E.R.C.; project administration, N.A.K. All authors have read and agreed to the published version of the manuscript.

Funding: This research was funded by the Russian Ministry of Science and High Education via the Institute of Cytology and Genetics [State Budget Project No. FWNR-2022-0016], as well as Inga N. Zaitseva.

Institutional Review Board Statement: The study was conducted in accordance with the Declaration of Helsinki, and approved by the Local Ethics Committee of the Research Institute of Fundamental and Clinical Immunology (protocol No. 120 dated November 7, 2018).

Informed Consent Statement: Informed consent was obtained from all subjects involved in the study. Written informed consent has been obtained from the patients to publish this paper.

Data Availability Statement: The original contributions presented in the study are included in the article/supplementary material, further inquiries can be directed to the corresponding author.

Acknowledgments: The authors express their gratitude to the Common Use Center of Flow Cytometry IC&G SB RAS and the Common Use Center for Microscopy of Biologic Objects SB RAS.

Conflicts of Interest: The authors declare no conflicts of interest. The funders had no role in the design of the study; in the collection, analyses, or interpretation of data; in the writing of the manuscript; or in the decision to publish the results.

References

1. Riggio, A. I.; Varley, K. E.; Welm, A. L. The lingering mysteries of metastatic recurrence in breast cancer. *Br J Cancer* **2021**, *124*(1), 13–26.
2. Schepotin, I. B.; Zotov, A. S.; Lyubota, R. V.; Anikusko, N. F.; Lyubota, I. I. The clinical significance of breast cancer stem cells. *Tumors of the female reproductive system* **2014,** *3*, 14-19. In Russian.
3. Schatton, T.; Murphy, G. F.; Frank N. Y. et al. Identification of cells initiating human melanomas. *Nature* **2008**, *451*(7176), 345–349.
4. Shurin, G. V.; Tourkova, I. L.; Kaneno, R.; Shurin M. R. Chemotherapeutic Agents in Noncytotoxic Concentrations Increase Antigen Presentation by Dendritic Cells via an IL-12-Dependent Mechanism. *The Journal of Immunology* **2009**, *183*(1) 137–144.
5. Schofield, P.; Carey, M.; Love, A.; Nehill, C.; Wein S. 'Would you like to talk about your future treatment options?' Discussing the transition from curative cancer treatment to palliative care. *Palliat Med* **2006,** *20*(4), 397–406.
6. Kim W. T.; Ryu, C. J. Cancer stem cell surface markers on normal stem cells. *BMB Rep* **2017**, *50*(6), 285–298.

Preprints.org (www.preprints.org) | NOT PEER-REVIEWED | Posted: 25 September 2024 doi:10.20944/preprints202409.2002.v

7. Schito, L.; Rey, S.; Xu, P. et al. Metronomic chemotherapy offsets HIFα induction upon maximum-tolerated dose in metastatic cancers. *EMBO Mol Med* **2020**, *12*(9).
8. Sell, S. Alpha-fetoprotein, stem cells and cancer: how study of the production of alpha-fetoprotein during chemical hepatocarcinogenesis led to reaffirmation of the stem cell theory of cancer. *Tumour Biol* **2008**, *29*(3), 161–180.
9. Takeda, K.; Mizushima, T., Yokoyama, Y. et al. Sox2 is associated with cancer stem-like properties in colorectal cancer. *Sci Rep*, **2018**, *8*(1).
10. Wicha, M. S. Cancer stem cell heterogeneity in hereditary breast cancer. *Breast Cancer Research* **2008**, *10*(2), 105.
11. Tashireva, L. A.; Perelmuter, V. M.; Manskikh, V. N. et al. Types of immune-inflammatory responses as a reflection of cell–cell interactions in tissue regeneration and tumor growth. *Biochemistry (Moscow)* **2017**, *82*(5), 732–748. In Russian.
12. van Cutsem, E.; Nordlinger, B.; Cervantes, A. Advanced colorectal cancer: ESMO clinical practice guidelines for treatment. *Annals of Oncology* **2010**, *21*(SUPPL. 5), v93-97.
13. Wang, J.; Liu, X.; Jiang, Z. et al. A novel method to limit breast cancer stem cells in states of quiescence, proliferation or differentiation: Use of gel stress in combination with stem cell growth factors. *Oncol Lett* **2016**, *12*(2), 1355–1360.
14. Wright, M. H., Calcagno, A. M., Salcido, C. D. et al. Brca1 breast tumors contain distinct CD44+/CD24- and CD133+ cells with cancer stem cell characteristics. *Breast Cancer Res* **2008**, *10*(1), R10.
15. Su, J.; Wu, S.; Wu, H.; Li, L.; Guo, T. CD44 is functionally crucial for driving lung cancer stem cells metastasis through Wnt/β-catenin-FoxM1-Twist signaling. *Mol Carcinog* **2016**, *55*(12), 1962–1973.
16. Wu, C.; Wei, Q.; Utomo, V. et al. Side population cells isolated from mesenchymal neoplasms have tumor initiating potential. *Cancer Res* **2007**, *67*(17), 8216–8222.
17. Wu J.; Waxman, D. J. Metronomic cyclophosphamide eradicates large implanted GL261 gliomas by activating antitumor Cd8 $^+$ T-cell responses and immune memory. *Oncoimmunology* **2015**, *4*(4), e1005521.
18. Yilmaz O. H.; Morrison, S. J. The PI-3kinase pathway in hematopoietic stem cells and leukemia-initiating cells: a mechanistic difference between normal and cancer stem cells. *Blood Cells Mol Dis* **2008**, *41*(1), 73–76.
19. Yang, Z. F.; Ho, D. W.; Ng, M. N. et al. Significance of CD90+ Cancer Stem Cells in Human Liver Cancer. *Cancer Cell* **2008**, *13*(2), 153–166.
20. Murakawa, Y.; Sakayori, M.; Otsuka, K. Impact of palliative chemotherapy and best supportive care on overall survival and length of hospitalization in patients with incurable Cancer: a 4-year single institution experience in Japan. *BMC Palliat Care* **2019**, *18*(1).
21. Yin, T.; Wei, H.; Gou, S. et al. Cancer stem-like cells enriched in Panc-1 spheres possess increased migration ability and resistance to gemcitabine. *Int J Mol Sci* **2011**, *12*(3), 1595–1604.
22. Barker, N.; Ridgway, R. A.; Van Es, J. H. et al. Crypt stem cells as the cells-of-origin of intestinal cancer. *Nature* **2009**, *457*(7229), 608–611.
23. Yin, W.; Wang, J.; Jiang, L.; James Kang, Y. Cancer and stem cells. *Exp Biol Med (Maywood)* **2021**, *246*(16), 1791–1801.
24. Yu, F.; Yao, H.; Zhu, P. et al. let-7 regulates self renewal and tumorigenicity of breast cancer cells. *Cell* **2007**, *131*(6), 1109–1123.
25. Garcia-Mayea, Y., Mir, C.; Masson, F.; Paciucci, R.; LLeonart, M. E. Insights into new mechanisms and models of cancer stem cell multidrug resistance. *Semin Cancer Biol* **2020**, *60*, 166–180.
26. Yuan, F.; Shi, H.; Ji, J. et al. Capecitabine metronomic chemotherapy inhibits the proliferation of gastric cancer cells through anti-angiogenesis. *Oncol Rep* **2015**, *33*(4), 1753–1762.
27. Zhang, Z.; Zhang, X.; Newman, K.; Liu, X. MicroRNA regulation of oncolytic adenovirus 6 for selective treatment of castration-resistant prostate cancer. *Mol Cancer Ther* **2012**, *11*(11), 2410–2418.
28. Badalyan, G. Kh.; Badalyan, L. G. Evaluation of the effectiveness of palliative chemotherapy depending on the intensity of treatment regimens. *Eurasian Journal of Oncology* **2012**, *2*, 413–413.
29. Eramo, A.; Lotti, F.; Sette G. et al. Identification and expansion of the tumorigenic lung cancer stem cell population. *Cell Death Differ* **2008**, *15*(3), 504–514.
30. Hu Y.; Smyth, G. K. ELDA: extreme limiting dilution analysis for comparing depleted and enriched populations in stem cell and other assays. *J Immunol Methods* **2009**, *347*(1–2), 70–78.
31. Ruzanova, V.; Proskurina, A.; Efremov, Y. et al. Chronometric Administration of Cyclophosphamide and a Double-Stranded DNA-Mix at Interstrand Crosslinks Repair Timing, Called 'Karanahan' Therapy, Is Highly Efficient in a Weakly Immunogenic Lewis Carcinoma Model. *Pathol Oncol Res* **2022**, *28*: 1610180.
32. Proskurina, A. S.; Kupina, V. V.; Efremov, Y. R. et al. Karanahan: a potential new treatment option for human breast cancer and its validation in a clinical setting. *Breast Cancer: Basic and Clinical Research* **2022**, *16*.
33. Potter, E. A.; Dolgova, E. V.; Proskurina, A. S. et al. A strategy to eradicate well-developed Krebs-2 ascites in mice. *Oncotarget* **2016**, *7*(10), 11580–11594.

Preprints.org (www.preprints.org) | NOT PEER-REVIEWED | Posted: 25 September 2024 doi:10.20944/preprints202409.2002.v

34. Potter, E. A.; Proskurina, A. S.; Ritter, G. S. et al. Efficacy of a new cancer treatment strategy based on eradication of tumor-initiating stem cells in a mouse model of Krebs-2 solid adenocarcinoma. *Oncotarget* **2018**, *9*(47), 28486–28499.
35. Potter, E. A.; Ritter, G. S.; Dolgova, E. V. et al. Evaluating the efficiency of the tumor-initiating stem cells eradication strategy on the example of ascite form of mouse gepatocarcinoma G-29. *Problems in Oncology* **2018**, *64*(6), 818–829. In Russian.
36. Kisaretova, P. E.; Kirikovich, S. S.; Ritter, G. S. et al. Approbation of the cancer treatment approach based on the eradication of TAMRA+ cancer stem cells in a model of murine cyclophosphamide resistant lymphosarcoma. *Anticancer Res* **2020**, *40*(2), 795–805.
37. Ruzanova, V.; Proskurina, A.; Ritter, G. et al. Experimental comparison of the in vivo efficacy of two novel anticancer therapies. *Anticancer Res* **2021**, *41*(7), 3371–3387.
38. Dolgova, E. V.; Potter, E. A.; Proskurina, A. S. et al. Evaluating the effectiveness of the tumor-initiating stem cells eradication strategy on the example of human glioblastoma cell line U87. *Problems in Oncology* **2019**, *65*(6), 904–919. In Russian.
39. Dolgova, E.; Andrushkevich, O.; Kisaretova, P. et al. Efficacy of the new therapeutic approach in curing malignant neoplasms on the model of human glioblastoma. *Cancer Biol Med*, **2021**, *18*(3), 910-930.
40. Proskurina, A. S.; Ruzanova, V. S.; Ostanin, A. A.; Chernykh, E. R.; Bogachev, S. S. Theoretical premises of a 'three in one' therapeutic approach to treat immunogenic and nonimmunogenic cancers: a narrative review. *Transl Cancer Res* **2021**, *10*(11), 4958–4972.
41. Dolgova, E. V.; Proskurina, A. S.; Nikolin, V. P. et al. 'Delayed death' phenomenon: A synergistic action of cyclophosphamide and exogenous DNA. *Gene* **2012**, *495*(2), 134–145.
42. Dolgova, E. V.; Efremov, Y. R.; Orishchenko, K. E. et al. Delivery and processing of exogenous double-stranded DNA in mouse CD34+ hematopoietic progenitor cells and their cell cycle changes upon combined treatment with cyclophosphamide and double-stranded DNA. *Gene* **2013**, *528*(2), 74–83.
43. Dolgova, E. V.; Alyamkina, E. A.; Efremov, Y. R. et al. Identification of cancer stem cells and a strategy for their elimination. *Cancer Biol Ther* **2014**, *15*(10), 1378–1394.
44. Alyamkina, E. A.; Nikolin, V. P.; Popova, N. A. et al. Combination of cyclophosphamide and double-stranded DNA demonstrates synergistic toxicity against established xenografts. *Cancer Cell Int* **2015**, *15*, 32.
45. Salavaty, A.; Azadian, E.; Naik, S. H.; Currie, P. D. Clonal selection parallels between normal and cancer tissues. *Trends Genet* **2023**, *39*(5), 358–380.
46. Greaves, M.; Maley, C. C. Clonal evolution in cancer. *Nature* **2012**, *481*(7381), 306–313.
47. Dolgova, E. V.; Rogachev, V. A.; Nikolin, V. P. et al. A leukocyte-stimulating effect of exogenous DNA fragments protected with protamine in the cyclophosphamide-induced myelosuppression in mice. *Problems in Oncology* **2009**, *55*(6), 761–764. In Russian.

Disclaimer/Publisher's Note: The statements, opinions and data contained in all publications are solely those of the individual author(s) and contributor(s) and not of MDPI and/or the editor(s). MDPI and/or the editor(s) disclaim responsibility for any injury to people or property resulting from any ideas, methods, instructions or products referred to in the content.